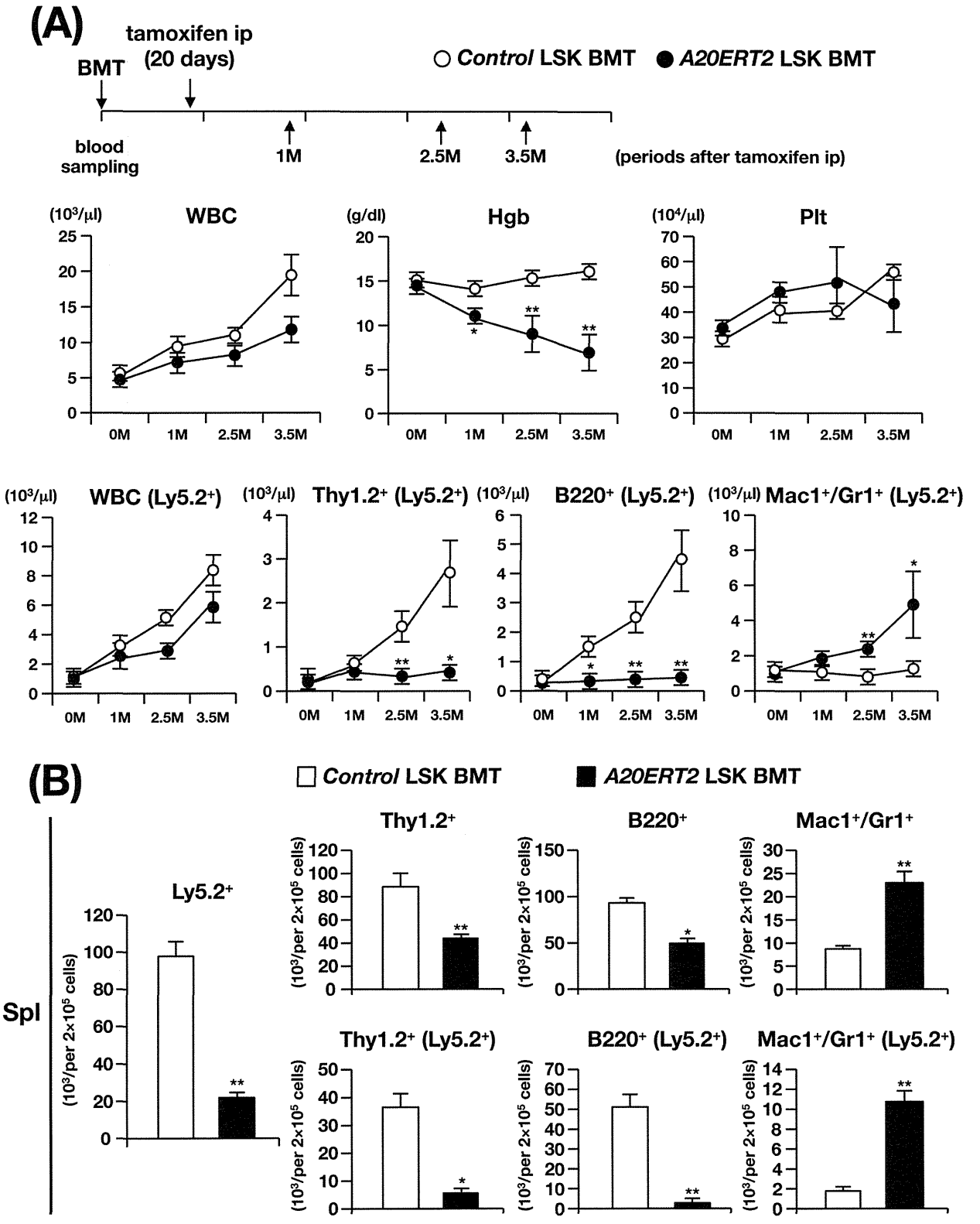

Figure 5. Analysis of *control* and *A20ERT2* LSK BMT mice. (A) Time schedule of BMT, tamoxifen ip, blood sampling, and time-dependent changes of hematopoietic parameters and percentages of Ly5.2$^+$ cells in the PB. *p<0.05 and **p<0.01 (Student's *t*-test). (B) Percentages of different hematopoietic compartments and the population of Ly5.2$^+$ cells in the spleen 3.5 M after transplantation. **p<0.01 (Student's *t*-test).
doi:10.1371/journal.pone.0087425.g005

characteristic for HSCs to maintain their stemness and engraftment activity. Our findings in this regard are consistent with those of previous studies demonstrating that cycling HSCs lose its repopulating ability [32,33,34]. Whether HSCs sense and directly respond to inflammation is controversial [35,36]. Our results suggest that HSCs could be a direct target of systemic inflammation and support the idea that TNF-α and IFN-γ are major regulators of inflammatory responses of HSCs, as documented in previous studies [34,37].

Next, we used *ERT2Cre* mice that respond to exogenously administered tamoxifen but not to endogenous estrogens. As expected, unlike *A20Mx* mice, *A20ERT2* mice did not exhibit an abnormal phenotype before tamoxifen stimulation. However, tamoxifen administration induced rapid death of the *A20ERT2* mice, which we attribute to severe apoptosis (Fig. S4). Moreover, there was a marked decrease in the numbers of hematopoietic cells in *A20ERT2* BMT mice following tamoxifen treatment (Fig. 4). These results indicate that loss of A20 induces rapid systemic apoptosis of hematopoietic cells.

The roles of A20 in apoptosis differ among published studies. For example, certain A20 deficient cells such as fibroblasts, splenocytes, and enterocytes exhibit enhanced sensitivity to TNF-α-mediated apoptosis [6,20]. In contrast, re-expressing A20 in A20 deficient lymphoma cells promotes apoptosis [7,8]. These findings indicate that A20 might play reciprocal roles in cell survival and cell death, depending on the cell types and cell contexts. Accordingly, our present results demonstrate that acquired A20 deficiency induces fulminant apoptosis in all cell types, including hematopoietic cells. This suggests that A20 primarily prevents apoptosis in adult tissues. There is evidence that the interaction of A20 with caspase-8 might play a role in this process [38].

The features shared by *A20ERT2* and *A20ERT2* LSK BMT included an increase in the number of myeloid cells, a decrease in the number of lymphocytes, and anemia, and similar to those of *A20Mx* and *A20Mx* BMT mice (Figs. 1, 2, 4, and 5). Thus, cytokine synthesis by hematopoietic cells that survived the apoptotic stage was uncontrolled and caused fulminant inflammation. Proliferation of myeloid cells would be a direct effect of increased production of pro-inflammatory cytokines, and anemia would be attributed to inflammation-induced impaired erythropoiesis as previously described [39]. In contrast, the mechanism responsible for reducing lymphocyte numbers, particularly those of B cells, remains to be clarified. Pathological analysis revealed that B lymphocytes underwent apoptosis in the spleen (Fig. S3), in contrast to previous reports, which show that in B cell-specific A20 deficient mice, B lymphocytes were hyper-reactive to exogenous stimuli and resistant to apoptosis [15,16,17]. The mechanism(s) underlying this discrepancy is unknown. One possibility is that B cell behaviors in response to A20 deficiency might differ, depending on the developmental stages at which A20 is deleted (namely, in B lineage-committed cells or in more primitive cells including HSCs). Another possibility is that death factor(s) secreted by systemic inflammation, such as TNF-α might affect lymphocytes and induce apoptosis.

The role of A20 in B cell development/differentiation is of particular interest, because hematopoietic malignancies with A20 mutations are exclusively B lineage lymphomas [7,8]. Mice with deletions of *A20* in the B lineage cells exhibit autoimmune-like diseases but fail to develop lymphoproliferative disorders [15,16,17]. Moreover, MALT lymphoma, a subtype of B-cell lymphoma in which A20 is frequently mutated, originates from mutated hematopoietic stem–early progenitor cells [40]. Therefore, A20 function must be abrogated in early progenitor cells to mimic B-cell lymphomas harboring *A20* mutations, as accomplished here. However, because apoptosis decreased the number of B cells in *A20Mx* and *A20ERT2* mice (Figs. S3 and S4), anti-apoptotic signal(s) might be necessary to exhibit a fully malignant phenotype. To address this possibility, we are crossing *A20Mx* mice with *p53* knockout mice to prevent apoptosis, and with *CagA* transgenic mice, a model for *Helicobactor pylori* infection that plays a pivotal role in the initiation of MALT lymphoma [41].

In summary, we generated mice in which *A20* can be inducibly and preferentially deleted from hematopoietic cells and found that acquired loss of A20 induced fulminant apoptosis and subsequent systemic inflammation. Our results demonstrate the essential role of A20 in the maintenance of adult hematopoietic cell homeostasis and provide insights into the mechanism responsible for A20 dysfunction and human diseases with *A20* mutations.

Supporting Information

Figure S1 Generation of *A20* conditional knockout mice. (A) Targeting strategy. Exon 3 of mouse *A20* was *floxed* and the *Frt*-flanked *Neo*-resistance gene was removed using Flp recombinase. The positions of a 5′ probe for Southern blotting and P1 and P2 primers for 3′ genomic PCR analysis are shown. Restriction sites: *Ba*, *BamH*I; *Sac*, *Sac*I; *Stu*, *Stu*I; *Sal*, *Sal*I; *Bg*, *Bgl*II. (B) Southern blotting and genomic PCR using a 5′ probe and 3′ primers, respectively, to detect homologous recombination in two dependent ES clones (#1 and #2). Germline (GL) and targeted allele-derived bands are indicated by arrows (left panel), and the recombination-specific PCR product is indicated by an arrowhead (right panel). (C) Western blotting of A20 expression in $A20^{flox/flox}$ $MxCre^{+}$ mice. Proteins extracted from the spleens of LPS-stimulated $A20^{flox/flox}$ $MxCre^{-}$ and $A20^{flox/flox}$ $MxCre^{+}$ mice were blotted and probed with anti-A20- (upper panel) or anti-β-actin antibodies (lower panel). The position of A20 is indicated by an arrow.
(PDF)

Figure S2 Proliferation of mature myeloid cells in the spleen of *A20Mx* and *A20Mx* BMT mice. Higher magnification of HE-stained sections of the spleen of *A20Mx* and *A20Mx* BMT mice. Mature myeloid cells with segmented or multi-lobulated nuclei are indicated by arrowheads.
(PDF)

Figure S3 Apoptosis of B cells. Representative results of double staining with an anti-B cell antibody and TUNEL in *control* and *A20Mx* spleens (three weeks old). Blue and brown staining patterns show B and apoptotic cells, respectively. The boxed areas in the upper panels are magnified in the lower panels.
(PDF)

Figure S4 Analysis of *control* and *A20ERT2* mice. (A) HE-stained *A20ERT2* tissues that show severe apoptosis. Microemboli and necrotic areas in the liver are indicated by arrowheads and an arrow, respectively. § below standard range and out of invertable range. (B) Serum concentrations of pro-inflammatory cytokines. *$p<0.05$ and **$p<0.01$ (Student's *t*-test). § below standard range and out of invertable range.
(PDF)

Figure S5 Colony formation assay. (A) The colony numbers generated in the presence of SCF+IL3+Epo, and those generated with SCF+IL7 are shown. No significant difference was observed between *control* and *A20Mx* mice. (B) Representative images of colonies. Colonies derived from both types of mice are similar in size and shape.
(PDF)

Table S1 Antibodies. All the antibodies used in this study are listed.
(PDF)

Table S2 Characteristics of *A20Mx* mice. Hematopoietic parameters of moribund *A20Mx* mice are described.
(PDF)

Text S1 Construction of a targeting vector and generation of *A20* knockout mice. Detailed procedure of Construction of a targeting vector and generation of *A20* knockout mice is described.
(PDF)

References

1. Ghosh S, Hayden MS (2008) New regulators of NF-kappaB in inflammation. Nat Rev Immunol 8: 837–848.
2. Shembade N, Harhaj EW (2012) Regulation of NF-κB signaling by the A20 deubiquitinase. Cell Mol Immunol 9: 123–130.
3. DiDonato JA, Mercurio F, Karin M (2012) NF-κB and the link between inflammation and cancer. Immunol Rev 246: 379–400.
4. Hymowitz SG, Wertz IE (2010) A20: from ubiquitin editing to tumour suppression. Nat Rev Cancer 10: 332–341.
5. Ma A, Malynn BA (2012) A20: linking a complex regulator of ubiquitylation to immunity and human disease. Nat Rev Immunol 12: 774–785.
6. Lee EG, Boone DL, Chai S, Libby SL, Chien M, et al. (2000) Failure to regulate TNF-induced NF-kappaB and cell death responses in A20-deficient mice. Science 289: 2350–2354.
7. Kato M, Sanada M, Kato I, Sato Y, Takita J, et al. (2009) Frequent inactivation of A20 in B-cell lymphomas. Nature 459: 712–716.
8. Compagno M, Lim WK, Grunn A, Nandula SV, Brahmachary M, et al. (2009) Mutations of multiple genes cause deregulation of NF-kappaB in diffuse large B-cell lymphoma. Nature 459: 717–721.
9. Graham RR, Cotsapas C, Davies L, Hackett R, Lessard CJ, et al. (2008) Genetic variants near TNFAIP3 on 6q23 are associated with systemic lupus erythematosus. Nat Genet 40: 1059–1061.
10. Musone SL, Taylor KE, Lu TT, Nititham J, Ferreira RC, et al. (2008) Multiple polymorphisms in the TNFAIP3 region are independently associated with systemic lupus erythematosus. Nat Genet 40: 1062–1064.
11. Adrianto I, Wen F, Templeton A, Wiley G, King JB, et al. (2011) Association of a functional variant downstream of TNFAIP3 with systemic lupus erythematosus. Nat Genet 43: 253–258.
12. Plenge RM, Cotsapas C, Davies L, Price AL, de Bakker PI, et al. (2007) Two independent alleles at 6q23 associated with risk of rheumatoid arthritis. Nat Genet 39: 1477–1482.
13. Thomson W, Barton A, Ke X, Eyre S, Hinks A, et al. (2007) Rheumatoid arthritis association at 6q23. Nat Genet 39: 1431–1433.
14. Consortium WTCC (2007) Genome-wide association study of 14,000 cases of seven common diseases and 3,000 shared controls. Nature 447: 661–678.
15. Tavares RM, Turer EE, Liu CL, Advincula R, Scapini P, et al. (2010) The ubiquitin modifying enzyme A20 restricts B cell survival and prevents autoimmunity. Immunity 33: 181–191.
16. Chu Y, Vahl JC, Kumar D, Heger K, Bertossi A, et al. (2011) B cells lacking the tumor suppressor TNFAIP3/A20 display impaired differentiation and hyperactivation and cause inflammation and autoimmunity in aged mice. Blood 117: 2227–2236.
17. Hövelmeyer N, Reissig S, Xuan NT, Adams-Quack P, Lukas D, et al. (2011) A20 deficiency in B cells enhances B-cell proliferation and results in the development of autoantibodies. Eur J Immunol 41: 595–601.
18. Kool M, van Loo G, Waelput W, De Prijck S, Muskens F, et al. (2011) The ubiquitin-editing protein A20 prevents dendritic cell activation, recognition of apoptotic cells, and systemic autoimmunity. Immunity 35: 82–96.
19. Matmati M, Jacques P, Maelfait J, Verheugen E, Kool M, et al. (2011) A20 (TNFAIP3) deficiency in myeloid cells triggers erosive polyarthritis resembling rheumatoid arthritis. Nat Genet 43: 908–912.
20. Vereecke L, Sze M, Mc Guire C, Rogiers B, Chu Y, et al. (2010) Enterocyte-specific A20 deficiency sensitizes to tumor necrosis factor-induced toxicity and experimental colitis. J Exp Med 207: 1513–1523.
21. Kuhn R, Schwenk F, Aguet M, Rajewsky K (1995) Inducible gene targeting in mice. Science 269: 1427–1429.
22. Miyamoto K, Miyamoto T, Kato R, Yoshimura A, Motoyama N, et al. (2008) FoxO3a regulates hematopoietic homeostasis through a negative feedback pathway in conditions of stress or aging. Blood 112: 4485–4493.

Acknowledgments

We thank Yuki Sakai, Yu Iwai, Sawako Ogata, and Rika Tai for animal care, genotyping, and molecular experiments. We also thank Dr. Junji Takeda of Osaka University and the RIKEN BioResource Center in Japan for providing us with KY1.1 ES cells and B6-Tg(CAG-FLPe)36 mice (RBRC01834), respectively. We express our sincere gratitude to Kalmia Caravan for encouragement and emotional support.

Author Contributions

Conceived and designed the experiments: AN ZH TS TI HH. Performed the experiments: AN TU NY YE K. Tsuji K. Takubo HO HH. Analyzed the data: AN YN TU NY YE K. Tsuji HO HH. Wrote the paper: TU YE K. Takubo HH.

23. Yamasaki N, Miyazaki K, Nagamachi A, Koller R, Oda H, et al. (2010) Identification of Zfp521/ZNF521 as a cooperative gene for E2A-HLF to develop acute B-lineage leukemia. Oncogene 29: 1963–1975.
24. Honda H, Takubo K, Oda H, Kosaki K, Tazaki T, et al. (2011) Hemp, an mbt domain-containing protein, plays essential roles in hematopoietic stem cell function and skeletal formation. Proc Natl Acad Sci USA 108: 2468–2473.
25. Nagamachi A, Htun PW, Ma F, Miyazaki K, Yamasaki N, et al. (2010) A 5′ untranslated region containing the IRES element in the Runx1 gene is required for angiogenesis, hematopoiesis and leukemogenesis in a knock-in mouse model. Dev Biol 345: 226–236.
26. Sinclair A, Daly B, Dzierzak E (1996) The Ly-6E.1 (Sca-1) gene requires a 3′ chromatin-dependent region for high-level gamma-interferon-induced hematopoietic cell expression. Blood 87: 2750–2761.
27. Kiel MJ, Yilmaz OH, Iwashita T, Yilmaz OH, Terhorst C, et al. (2005) SLAM family receptors distinguish hematopoietic stem and progenitor cells and reveal endothelial niches for stem cells. Cell 7: 1109–1121.
28. Iwai K (2012) Diverse ubiquitin signaling in NF-κB activation. Trends Cell Biol 22: 355–364.
29. Mochizuki-Kashio M, Mishima Y, Miyagi S, Negishi M, Saraya A, et al. (3011) Dependency on the polycomb gene Ezh2 distinguishes fetal from adult hematopoietic stem cells. Blood 118: 6553–6561.
30. Tanaka S, Miyagi S, Sashida G, Chiba T, Yuan J, et al. (2012) Ezh2 augments leukemogenicity by reinforcing differentiation blockage in acute myeloid leukemia. Blood 120: 1107–1117.
31. Lippens S, Lefebvre S, Gilbert B, Sze M, Devos M, et al. (2011) Keratinocyte-specific ablation of the NF-κB regulatory protein A20 (TNFAIP3) reveals a role in the control of epidermal homeostasis. Cell Death Differ 18: 1845–1853.
32. Passegué E, Wagers AJ, Giuriato S, Anderson WC, Weissman IL (2005) Global analysis of proliferation and cell cycle gene expression in the regulation of hematopoietic stem and progenitor cell fates. J Exp Med 202: 1599–1611.
33. Rodriguez S, Chora A, Goumnerov B, Mumaw C, Goebel WS, et al. (2009) Dysfunctional expansion of hematopoietic stem cells and block of myeloid differentiation in lethal sepsis. Blood 114: 4064–4076.
34. Baldridge MT, King KY, Boles NC, Weksberg DC, Goodell MA (2010) Quiescent haematopoietic stem cells are activated by IFN-gamma in response to chronic infection. Nature 465: 793–797.
35. Baldridge MT, King KY, Goodell MA (2010) Inflammatory signals regulate hematopoietic stem cells. Trends Immunol 32: 57–65.
36. King KY, Goodell MA (2011) Inflammatory modulation of HSCs: viewing the HSC as a foundation for the immune response. Nat Rev Immunol 11: 685–692.
37. Rezzoug F, Huang Y, Tanner MK, Wysoczynski M, Schanie CL, et al. (2008) TNF-alpha is critical to facilitate hemopoietic stem cell engraftment and function. J Immunol 180: 49–57.
38. Jin Z, Li Y, Pitti R, Lawrence D, Pham VC, et al. (2009) Cullin3-based polyubiquitination and p62-dependent aggregation of caspase-8 mediate extrinsic apoptosis signaling Cell 137: 721–735.
39. Morceau F, Dicato M, Diederich M (2009) Pro-inflammatory cytokine-mediated anemia: regarding molecular mechanisms of erythropoiesis. Mediators Inflamm Volume 2009, Article ID 405016.
40. Vicente-Dueñas C, Fontán L, Gonzalez-Herrero I, Romero-Camarero I, Segura V, et al. (2012) Expression of MALT1 oncogene in hematopoietic stem/progenitor cells recapitulates the pathogenesis of human lymphoma in mice. Proc Natl Acad Sci USA 109: 10534–10539.
41. Ohnishi N, Yuasa H, Tanaka S, Sawa H, Miura M, et al. (2008) Transgenic expression of Helicobacter pylori CagA induces gastrointestinal and hematopoietic neoplasms in mouse. Proc Natl Acad Sci USA 105: 1003–1008.

OPEN ACCESS Freely available online

PLOS ONE

Robust and Highly-Efficient Differentiation of Functional Monocytic Cells from Human Pluripotent Stem Cells under Serum- and Feeder Cell-Free Conditions

Masakatsu D. Yanagimachi[1,4], Akira Niwa[1], Takayuki Tanaka[1], Fumiko Honda-Ozaki[1], Seiko Nishimoto[1], Yuuki Murata[3], Takahiro Yasumi[3], Jun Ito[1], Shota Tomida[1], Koichi Oshima[1], Isao Asaka[2], Hiroaki Goto[4], Toshio Heike[3], Tatsutoshi Nakahata[1], Megumu K. Saito[1]*

1 Department of Clinilcal Application, Center for iPS Cell Research and Application, Kyoto University, Kyoto, Japan, **2** Department of Fundamental Cell Technology, Center for iPS Cell Research and Application, Kyoto University, Kyoto, Japan, **3** Department of Pediatrics, Kyoto University Graduate School of Medicine, Kyoto, Japan, **4** Department of Pediatrics, Yokohama City University Graduate School of Medicine, Yokohama, Japan

Abstract

Monocytic lineage cells (monocytes, macrophages and dendritic cells) play important roles in immune responses and are involved in various pathological conditions. The development of monocytic cells from human embryonic stem cells (ESCs) and induced pluripotent stem cells (iPSCs) is of particular interest because it provides an unlimited cell source for clinical application and basic research on disease pathology. Although the methods for monocytic cell differentiation from ESCs/iPSCs using embryonic body or feeder co-culture systems have already been established, these methods depend on the use of xenogeneic materials and, therefore, have a relatively poor-reproducibility. Here, we established a robust and highly-efficient method to differentiate functional monocytic cells from ESCs/iPSCs under serum- and feeder cell-free conditions. This method produced $1.3\times10^6\pm0.3\times10^6$ floating monocytes from approximately 30 clusters of ESCs/iPSCs 5–6 times per course of differentiation. Such monocytes could be differentiated into functional macrophages and dendritic cells. This method should be useful for regenerative medicine, disease-specific iPSC studies and drug discovery.

Citation: Yanagimachi MD, Niwa A, Tanaka T, Honda-Ozaki F, Nishimoto S, et al. (2013) Robust and Highly-Efficient Differentiation of Functional Monocytic Cells from Human Pluripotent Stem Cells under Serum- and Feeder Cell-Free Conditions. PLoS ONE 8(4): e59243. doi:10.1371/journal.pone.0059243

Editor: Katriina Aalto-Setala, University of Tampere, Finland

Received August 14, 2012; **Accepted** February 13, 2013; **Published** April 3, 2013

Funding: Funding was provided by grants from the Ministry of Health, Labour and Welfare to TN, a grant from the Ministry of Education, Culture, Sports, Science and Technology (MEXT) to TN, grants from the Leading Project of MEXT to TN, a grant from Funding Program for World-Leading Innovative Research and Development on Science and Technology (FIRST Program) of Japan Society for the Promotion of Science (JSPS) to TN, grants from JSPS to TN and MKS, grants from the Takeda foundation, Mitsubishi Pharma Research Foundation and Suzuken memorial foundation to MKS and grants from Grants-in-Aid for Scientific Research from Japan Society for the Promotion of Science from the Ministry of Education, Culture, Sports, Science, and Technology of Japan to MDY. The funders had no role in study design, data collection and analysis, decision to publish, or preparation of the manuscript.

Competing Interests: The authors have declared that no competing interests exist.

* E-mail: msaito@cira.kyoto-u.ac.jp

Introduction

Monocytic lineage cells, such as monocytes, macrophages and dendritic cells (DCs), are central to immune responses and play key roles in various pathological conditions. [1–2] Monocytes are the myeloid progeny of hematopoietic stem/progenitor cells [3]; they are a type of mononuclear cell circulating in the bloodstream and act as gatekeepers in innate immunity. While they replenish macrophages and DCs, monocytes themselves respond to various inflammatory stimuli by migrating into inflamed tissues, phagocytosing pathological small particles and producing proinflammatory cytokines and chemokines. Therefore, monocytes not only contribute to host defense against pathogenic microorganisms, but are closely associated with the pathogenesis of chronic sterile inflammation. [4] Macrophages reside in tissues and robustly phagocytose microorganisms and cellular debris. One of the important hallmarks of monocytic lineage cells is their functional plasticity. In response to cytokines and microbial products, macrophages polarize into functionally distinct M1 and M2 cells. [5] Classically activated M1 macrophages are induced by interferon-γ (IFNγ), while alternatively activated M2 macrophages can be induced by IL-4 and IL-13. [2,5] M1 macrophages are generally characterized by high production of proinflammatory cytokines, while M2 are characterized by high production of anti-inflammatory cytokines. DCs are the most powerful antigen-presenting cells and have an indispensable role for the activation of T lymphocytes. Because of their ability to mediate communication between innate and acquired immunity, ex vivo expansion of DCs is expected to be a useful source of material for cancer immunotherapies, such as DC-based vaccines. [6–7] Moreover, recent reports of monocyte and/or DC deficiencies highlight the importance of understanding their development in humans. [8] However, there have been technical limitations for tracing the development of human monocytic cells, or for propagating them ex vivo.

Human embryonic stem cells (ESCs) and induced pluripotent stem cells (iPSCs) are undifferentiated pluripotent cells that can be propagated indefinitely. [9–11] The development of monocytic cells from these pluripotent cells is of particular interest because it would provide an unlimited source of these cells for clinical applications and the examination of disease pathologies. Although the methods for hematopoietic differentiation from ESCs/iPSCs

using embryonic body or feeder co-culture systems have already been established, [12] these methods usually depend on xenogeneic feeder cells and/or animal- or human-derived serum, and therefore have a relatively poor-reproducibility. For instance, batch-to-batch variability of serum or feeder cells can influence the characteristics of *in vitro* differentiated DCs. [13] Here, we describe a novel serum- and feeder cell-free method that robustly and repetitively produces monocytic lineage cells from human ESCs/iPSCs.

Materials and Methods

Cell Culture

This study used human ESCs (cell line: KhES1) and iPSCs (cell lines: 201B7, 253G4, CIRA188Ai-W2, and CB-A11). [10,14–15] 201B7, 253G4 [10] and CIRA188Ai-W2 [15] were previously described. A human ES cell line KhES1 was kindly provided by Dr. Norio Nakatsuji. Human iPS cell lines 201B7 and 253G4 were kindly provided by Dr. Shinya Yamanaka. CB-A11 was established from cord-blood mononuclear cells by using episomal vectors. [16] These ESCs/iPSCs were maintained on tissue culture dishes coated with growth factor-reduced Matrigel (Becton-Dickinson) in mTeSR1 serum-free medium (STEMCELL Technologies).

Monocytic Lineage Cell Differentiation Method

The monocytic lineage differentiation protocol was modified from a previously established hematopoietic differentiation protocol (Figure 1). [17] The protocol consists of 5 sequential steps by which mature MPs and DCs are differentiated from human pluripotent cells in a stepwise manner. In the first step, primitive streak cells were induced from undifferentiated ESCs/iPSCs, which were then differentiated into hemangioblast-like hematopoietic progenitors in the second step. In step 3, expanded hematopoietic progenitors were committed towards initial myeloid differentiation, and then differentiated into the monocytic lineage in step 4. Finally, $CD14^+$ monocytes were differentiated into either MPs or DCs in step 5. The cytokines used in this study were purchased from R&D systems.

Step 1: induction of primitive streak-like cells from undifferentiated human ES/iPS cells with BMP4. BMP4 is an important molecule for the initial stage of mesodermal commitment of pluripotent stem cells in vitro. [17] Undifferentiated ESCs/iPSCs colonies were disseminated onto a 100 mm culture dish coated with growth factor-reduced Matrigel in mTeSR1 medium at a density of about 30 colonies per dish. Individual colonies were grown to a diameter of approximately 1 mm (Day 0), and BMP4 (80 ng/mL) was added to the mTeSR1 medium.

Step 2: generation of KDR^+CD34^+ hemangioblast-like cells with VEGF, basic FGF and SCF. VEGF and SCF have been reported to be important cytokines for development of hemoangiogenic progenitors. [18–19] In this step, we also added basic FGF which enhances the development of mesodermal hematopoietic progenitors. [18,20] The mTeSR1 medium was replaced by StemPro-34 serum-free medium (Gibco) containing 2 mM glutamax (Invitrogen) on day 4, and then was supplemented with the step-2 cytokine cocktail composed of VEGF (80 ng/mL), basic FGF (25 ng/ml), and SCF (100 ng/mL).

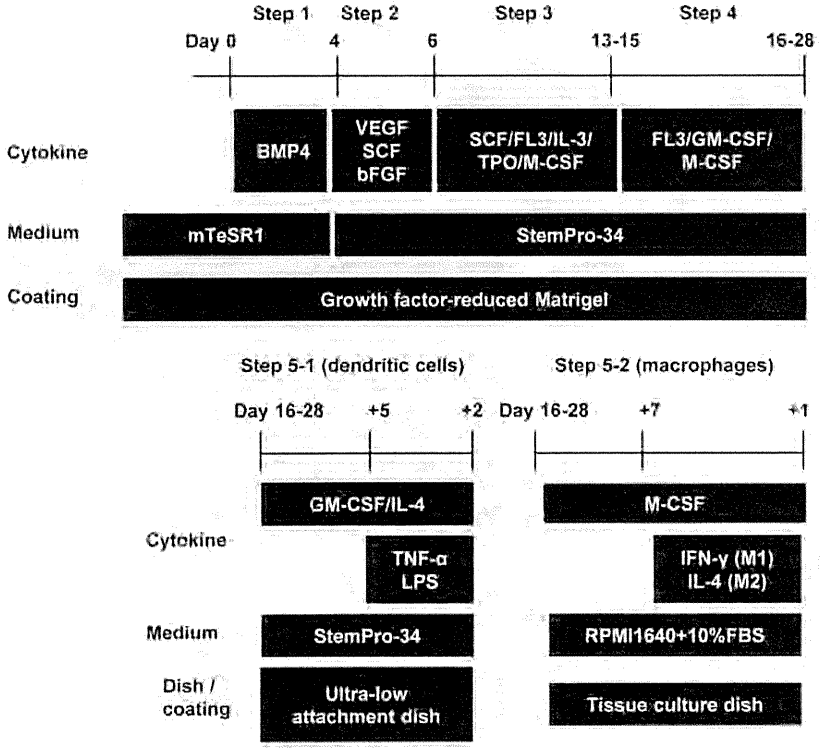

Figure 1. Protocol for monocytic lineage cell differentiation from human pluripotent stem cells. The protocol is composed of 5 steps. CD14-positive cells that are sorted between step-4 are differentiated into dendritic cells by step 5-1 or into macrophages by step 5-2. FL-3: Flt-3 ligand, TPO: Thrombopoietin.
doi:10.1371/journal.pone.0059243.g001

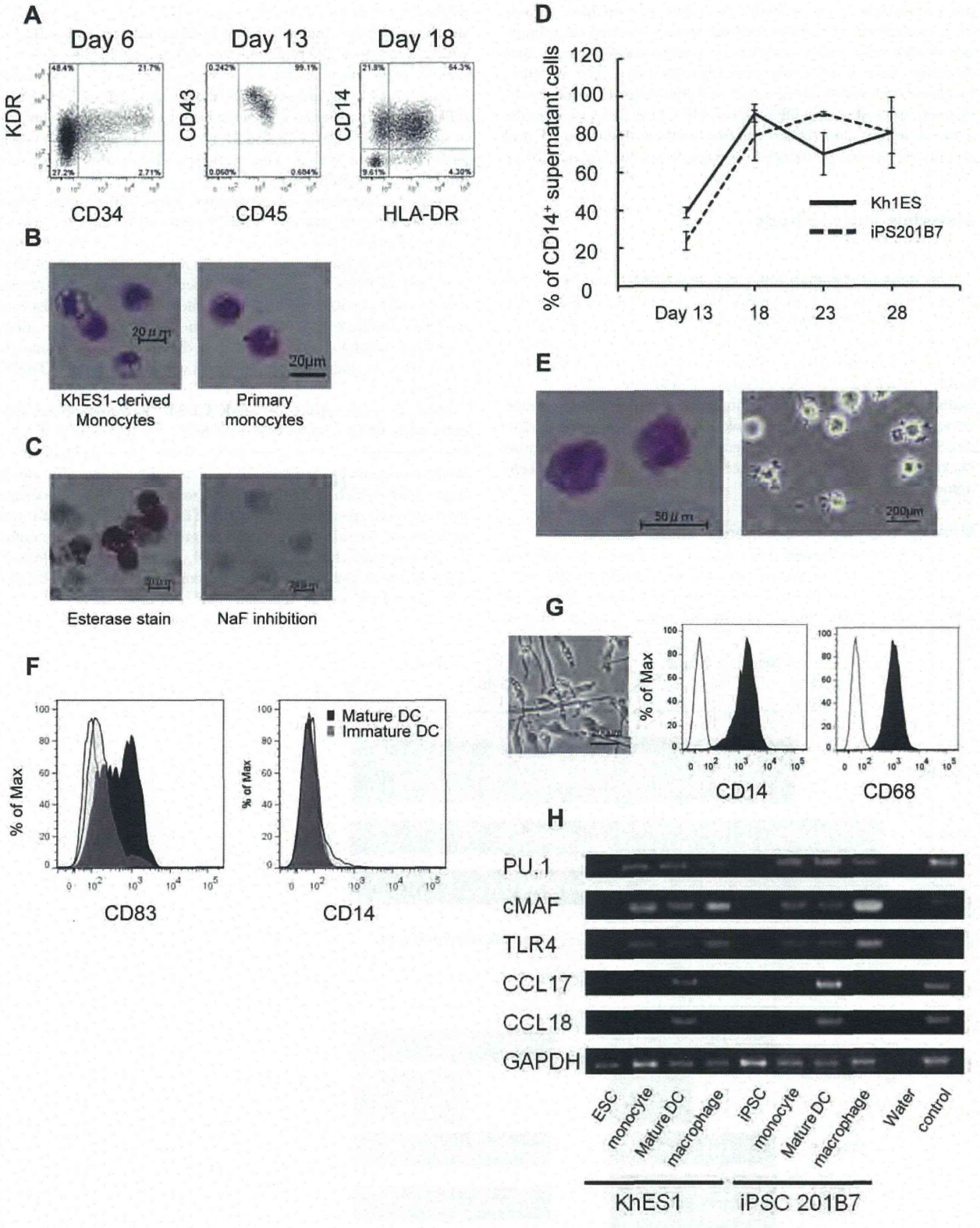

Figure 2. Phenotype analysis and gene expression pattern of monocytic lineage cells derived from pluripotent stem cells. (A) Flow cytometric analysis of monocytic lineage cells derived sequentially from pluripotent stem cells. An analysis of adherent cells on day 6 and supernatant cells on day 13 and 18 is shown. (B) May-Giemsa staining of $CD14^+$ monocyte-like cells derived from KhES1 on day 16 (left) and primary human monocytes (right). (C) Esterase staining for $CD14^+$ monocyte-like cells derived from KhES1 on day 16. (D) The percentage of $CD14^+$ cells within the total floating cells derived from KhES1/iPS-201B7 was evaluated from day 13 to day 28. (E) May-Giemsa staining (left) and phase contrast image (right)

of mature DCs derived from pluripotent stem cells. (F) Flow cytometric analysis of immature/mature DCs derived from pluripotent stem cells. (G) Phase contrast image and flow cytometric analysis of macrophages derived from pluripotent stem cells.(H) RT-PCR analysis of monocytic lineage cells derived from KhES1/iPS-201B7 clones for expression of monocytic lineage marker genes (*PU.1, c-MAF, TLR4, CCL17* and *CCL18*). Peripheral blood monocytes and peripheral blood monocyte-derived mature DCs were used as positive controls.(A–C, E–G) The data from KhES1-derived cells are shown as representative.
doi:10.1371/journal.pone.0059243.g002

Step 3: generation of hematopoietic cells with hematopoietic cytokines. The cytokines in StemPro-34 medium were switched to the step-3 cytokine cocktail composed of SCF (50 ng/mL), IL-3 (50 ng/mL), TPO (Thrombopoietin) (5 ng/mL), M-CSF (50 ng/mL), and Flt-3 ligand (50 ng/mL), on day 6. Thereafter, the medium was changed on day 10.

Step 4: monocytic lineage-directed differentiation with Flt-3 ligand, GM-CSF and M-CSF. The cytokines in StemPro-34 medium were switched to the step-4 cytokine cocktail composed of Flt-3 ligand (50 ng/mL), GM-CSF (25 ng/mL), and M-CSF (50 ng/mL) on day 13–15. The medium was changed every 3–4 days. The $CD14^+$ monocytic lineage-directed cell fraction in supernatant was positively sorted by autoMACS pro (Miltenyi Biotec) with CD14 MicroBeads (Miltenyi Biotec) on days 15–28.

Step 5: differentiation into DCs (step 5-1) and MPs (step 5-2) from $CD14^+$ monocytic lineage-cells. $CD14^+$ cells sorted by autoMACS pro (1.5×10^6 cells per well in a 6-well plate with Ultra-Low Attachment Surface (CORNING)) were cultured in StemPro-34 medium supplemented with GM-CSF (25 ng/mL) and IL-4 (40 ng/mL), with a medium change 4 days later, for differentiation into DCs (step 5-1). LPS (100 ng/mL, InvivoGen) and TNFα (0.2 ng/mL) were added for the last 2 days of the 7 day DC differentiation culture to promote maturation of DCs. $CD14^+$ cells (1.5×10^6 cells per well in a 6-well tissue culture plate) were cultured in RPMI-1640 medium (Sigma) supplemented with 10%

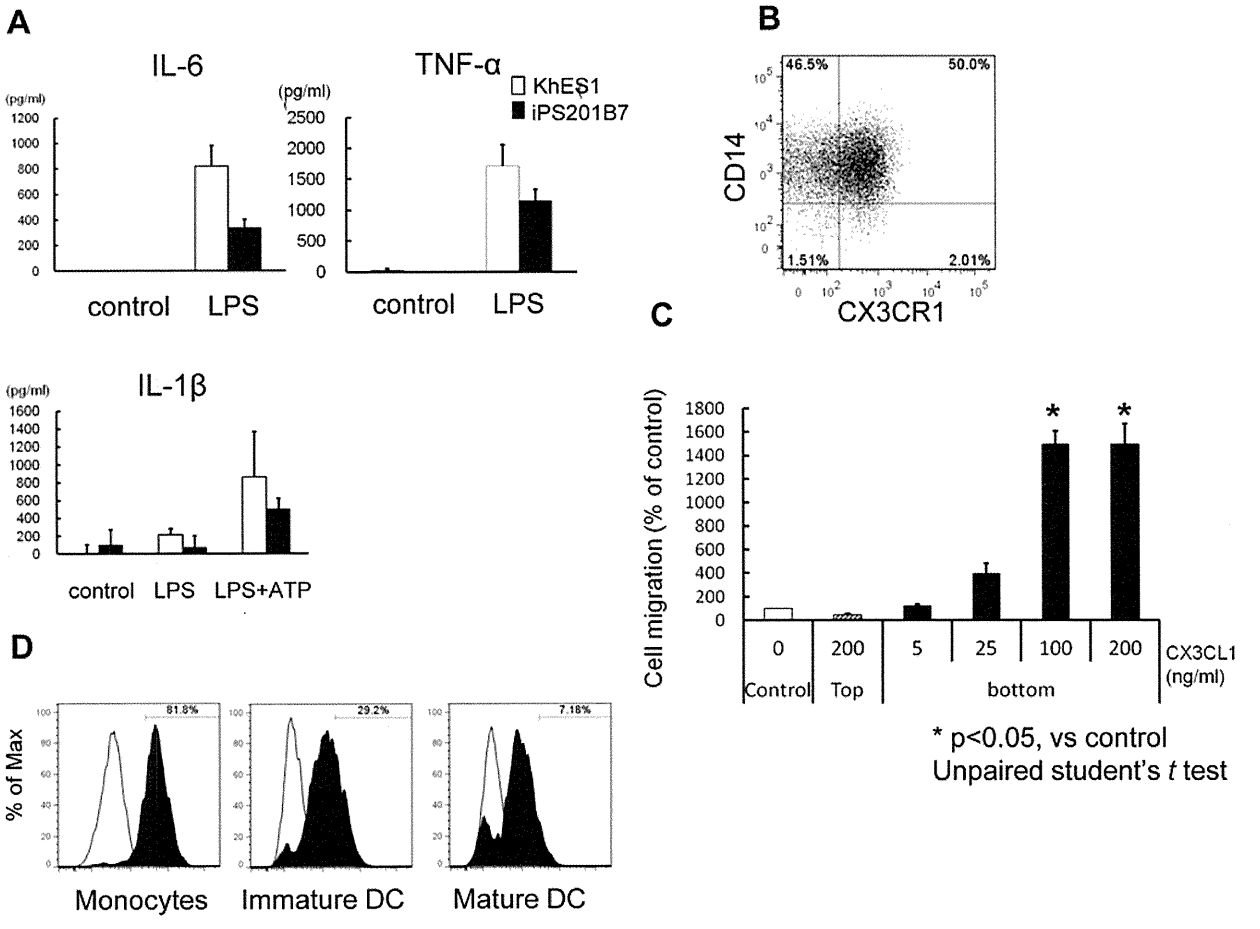

Figure 3. Functional assays for monocytes derived from pluripotent stem cells. (A) The levels of IL-6 and TNFα in supernatants of PS-Mo culture medium 4 hours after LPS stimulation. The levels of IL-1β were measured 4 hours after LPS stimulation with/without an additional 30-minute ATP stimulation. (B) Flow cytometric analysis of CX3CR1 on PS-Mo. (C) Chemotaxis assay of PS-Mo for CX3CL1 (fractalkine) using a trans-well migration assay. After the addition of CX3CL1 into either the bottom or top of the trans-well chamber, PS-Mo were applied and incubated for 5 hours at 37°C. (D) Antigen uptake was evaluated in monocytes, immature DCs and mature DCs derived from pluripotent stem cells by examining the fluorescence intensity of Alexa fluor 488-conjugated ovalbumin 45 minute after incubation at 37°C (black). Control samples (white) were kept on ice. (B–D) The data of KhES1-derived cells are shown as representative. PS-Mo: monocyte derived from pluripotent stem cells.
doi:10.1371/journal.pone.0059243.g003

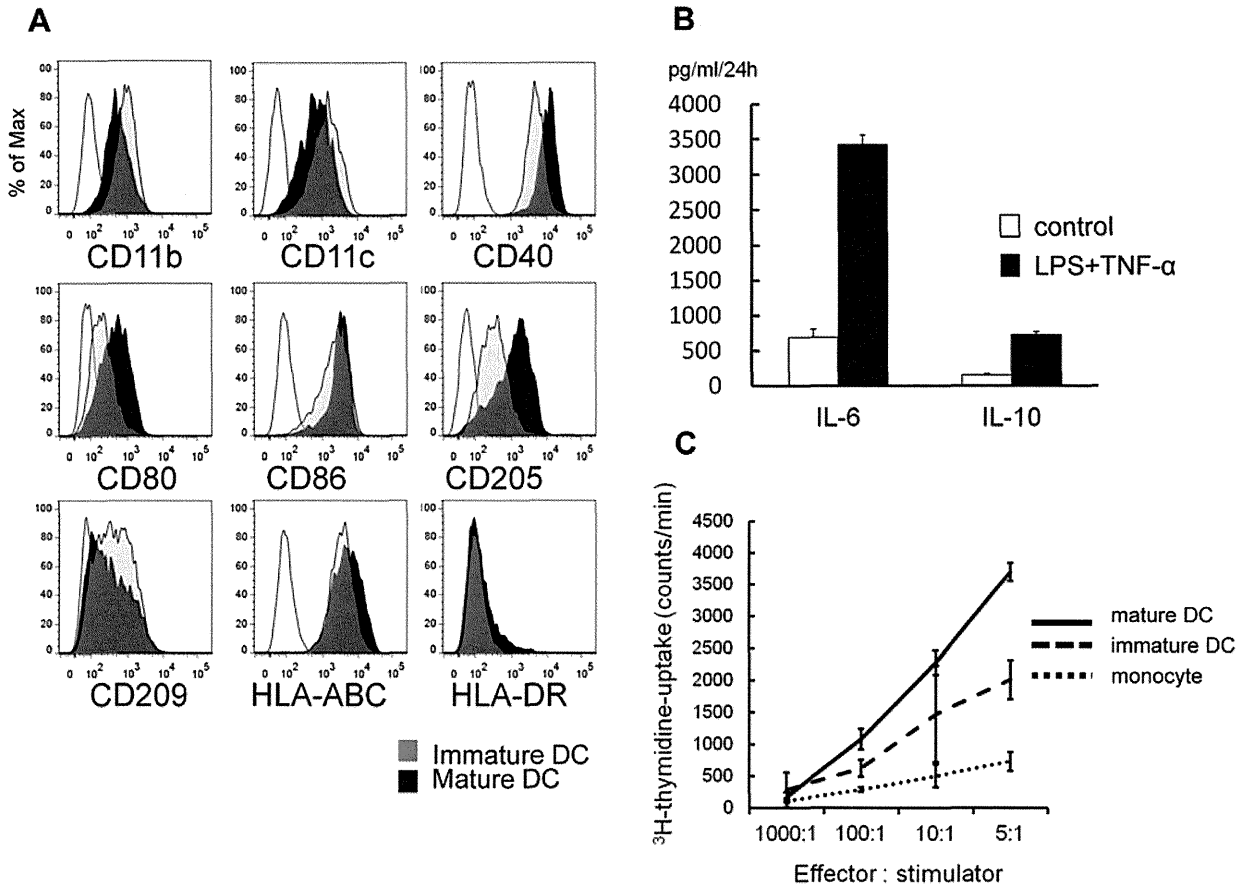

Figure 4. Functional assays for dendritic cells derived from pluripotent stem cells. (A) Flow cytometric analysis of immature/mature DCs derived from pluripotent stem cells. (B) The levels of IL-10 and TNFα in supernatants of culture medium with PS-DCs 24 hours after LPS stimulation. (C) The proliferation of allogeneic naïve T cells (1×10^5 cells per well) co-cultured with 40 Gy-irradiated stimulator cells for 3 days was evaluated. The proliferation of naïve T cells in the last 16 hours was measured by ^{3}H-thymidine uptake. (A–C) The data of KhES1-derived cells are shown as representative.
doi:10.1371/journal.pone.0059243.g004

fetal bovine serum (FBS) and M-CSF (100 ng/mL) for 7 days with a medium change at day 4, for differentiation into macrophages (step 5-2). IFNγ (20 ng/ml) or IL-4 (20 ng/ml) was added for another day to promote differentiation into M1 or M2 macrophages, respectively.

Flow Cytometric Analysis

Flow cytometric analysis data were collected using the MACS Quant™ Analyzer (Miltenyi Biotec) and then analyzed utilizing the FlowJo software package (Treestar). The following antibodies were purchased from BD Biosciences: CD11b-FITC, CD11c-APC, CD34-PE, CD40-PE, CD43-FITC, CD80-PE, CD83-PE, CD86-FITC, CD205-Alexa fluor 647, CD206-FITC, CD209-PE, HLA-ABC-FITC and HLA-DR-FITC. CD14-APC and CD45-APC antibodies were purchased from Beckman Coulter. CD163-APC antibody was purchased from R&D systems. KDR (CD309)-Alexa fluor 647 and CX3CR1-PE antibodies were purchased from Biolegend.

May-Giemsa Staining and Esterase Staining

Cells were seeded onto glass slides by CYTOSPIN 4 (Thermo Scientific) and stained with May-Grunwald and Giemsa staining solution (MERCK) and Esterase staining solution (Muto pure chemicals) following the manufacturer's instructions.

RNA Extraction and RT-PCR Analysis

RNA samples were prepared using the RNeasy mini kit (Qiagen) following the manufacturer's instructions. Typically, 500 ng of total RNA were subjected to reverse transcription (RT) with a Sensiscript-RT kit (Qiagen). RT-PCR was performed for the evaluation of the expression of monocytic lineage marker genes such as *PU.1, MAF, TLR4, CCL17* and *CCL18* using the primers in **Table S1**. [21–22] Peripheral blood monocyte-derived mature DCs/macrophages were generated from peripheral $CD14^+$ monocytes using the step 5-1/5-2 cytokine cocktails in 10% FBS-supplemented RPMI-1640 for use as positive controls.

Cytokine Assay

Concentrations of cytokines (IL-1β, IL-6, IL-10, IL-12p70 and TNFα) in supernatants were analyzed with FlowCytomix kits (Bender MedSystems) following the manufacturer's instructions. The IL-1β, IL-6 and TNFα levels in the culture supernatants of pluripotent cell-derived monocytes (PS-Mo) were analyzed in three settings, (1) culture in RPMI-1640 medium supplemented with 10% FBS and LPS (100 ng/ml) for 4.5 hours, (2) as in (1) but with

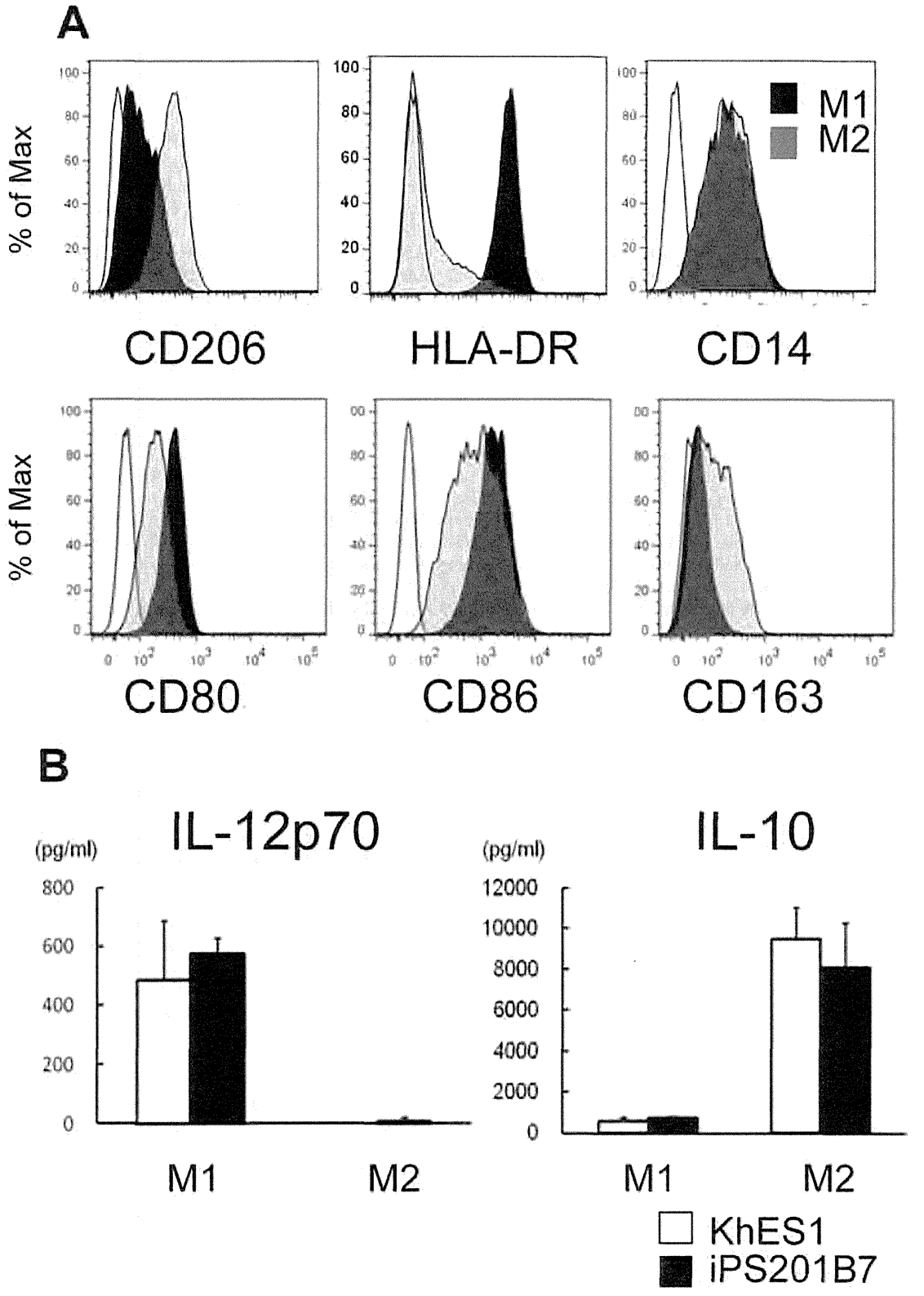

Figure 5. Functional assays for M1/M2 macrophages derived from pluripotent stem cells. (A) Flow cytometric analysis of M1/M2 macrophages derived from pluripotent stem cells. (B) The levels of IL-12p70 and IL-10 in supernatants of culture medium with M1/M2 macrophages derived from pluripotent stem cells 24 hours after LPS stimulation. The data of KhES1-derived cells are shown as representative.
doi:10.1371/journal.pone.0059243.g005

the addition of ATP (1 mM) for the last 30 min, (3) without LPS or ATP for 4.5 hours, to evaluate the production pattern of IL-1β in response to LPS plus ATP. [23].

The levels of IL-6, IL-10, IL-12p70 and TNFα in the supernatants of M1 or M2 macrophage culture were measured 24 hours after LPS (100 ng/ml) stimulation.

Chemotaxis Assay

PS-Mo chemotaxis was evaluated using a trans-well migration assay with 8-μm pore size inserts (BD Biosciences). After CX3CL1 (fractalkine; R&D systems) was added to either the bottom or top of the chamber, serum-starved PS-Mo were loaded onto the inserts which were placed into 24-well plates containing RPMI-1640 and then incubated at 37°C for 5 hours. [24] Cell migration was measured by flow cytometry as previously reported: equivalent amounts of counting beads were added to each sample and the ratios of PS-Mo to the counting beads were calculated. [25].

Antigen Uptake Assay

The antigen uptake capacity of monocytic lineage cells was evaluated as previously described. [26] Briefly, the cells were collected and stored on ice for 10 min. PS-Mo, pluripotent cell-derived immature DCs (PS-imDCs) and pluripotent cell-derived mature DCs (PS-mDCs) (5×10^4 cells) were incubated with Ovalbumin Alexa fluor 488 Conjugate (Molecular Probes) at 0.1 mg/ml at 37°C or on ice for 45 min. Ice-cold FACS buffer was added in order to stop the reaction, samples washed twice, and the fluorescence intensity analyzed by flow cytometry.

Mixed Leukocyte Reactions

Allogeneic naïve T cells (1×10^5 cells per well) were purified from umbilical cord blood mononuclear cells using naïve $CD4^+$ T cell isolation kits (Miltenyi Biotec) and then co-cultured with 40 Gy-irradiated stimulator cells (PS-Mo, PS-imDC, and PS-mDC) in 96-well round bottomed culture plates for 3–5 days. ^{3}H-methylthymidine (25 uCi/ml, Moravek Biochemicals and Radiochemicals) was added to the culture medium of 10% FBS-supplemented RPMI-1640 for the last 16 hours. The cells were harvested onto a filter mat (Perkin Elmer) and the ^{3}H methylthymidine uptake determined using a scintillation counter (MicroBeta TriLux, Perkin Elmer).

Ethical Considerations

This study was approved by the Ethics Committee of Kyoto University and written informed consent was obtained from each healthy volunteer.

Statistics

Data are presented as the mean ± S.D. and the statistical significance of the differences between cultures were evaluated by Student's *t*-test.

Results

Differentiation of ESCs/iPSCs into Dendritic Cells and Macrophages via Monocyte-like Cells

A KDR^+CD34^+ hemangioblast-like population was detected in adherent cell clusters on day 6 (steps 1,2), and around 95% of supernatant cells were $CD43^+CD45^+$ hematopoietic cells on days 13–15 (step 3; **Figure 2A**). [17] Floating cells were recovered every 3–4 days in step 4 (**Figure S1**); the majority of these cells were $CD14^+$ monocyte-like cells (**Figure 2A**). These pluripotent cell-derived monocytes (PS-Mo) were similar to peripheral blood monocytes in morphology (**Figure 2B**). PS-Mo are positive for Esterase staining which was inhibited by NaF (**Figure 2C**). The percentages of PS-Mo in floating cells were constantly about 50–90% between day 18–28 (**Figure 2D and Figure S2A**). The yield of PS-Mo per 100 mm culture dish starting with about 30 colonies was $1.3\times10^6\pm0.3\times10^6$ at each step-4 medium exchange.

To derive DCs, PS-Mo were purified by magnetic sorting, and differentiated into $CD14^-CD83^-$ immature DCs (PS-imDCs) with the step 5-1 cytokine cocktail in 5 days (**Figure 2E**). PS-imDCs were stimulated with LPS and TNFα for an additional 2 days, which further differentiated them into $CD14^-CD83^+$ mature DCs (PS-mDCs) (**Figure 2F**). The differentiation efficiency of mature DCs from PS-Mo was comparable to that from primary monocytes (7.7%±0.9% vs. 16.5%±1.0%, $p=0.20$, unpaired Student's *t*-test). PS-Mo also had the potential to differentiate into macrophages (PS-MPs) with the step 5-2 cytokine cocktail. PS-MPs are morphologically comparable to primary monocyte-derived macrophages and they express typical surface markers such as CD14 and CD68 (**Figure 2G and Figure S3A,B**).

We confirmed that PS-Mo, pluripotent cell-derived DCs (PS-DCs), and PS-MPs expressed monocytic lineage-specific genes (**Figure 2H and Figure S2B**). [22,27] Collectively, by using this protocol, sufficient numbers of monocytic cell lineage cells can be obtained from a small number of human ESCs/iPSCs.

Functional Assays for Monocytes Derived from ESCs/iPSCs

Next, we evaluated the functional activity of pluripotent cell-derived monocytic lineage cells. PS-Mo robustly produced the pro-inflammatory cytokines IL-6 and TNFα after LPS stimulation (**Figure 3A, Figure S3C**). Secretion pattern of IL-1β from PS-Mo with two stepwise signals LPS and ATP were similar to primary monocytes (**Figure 3A, Figure S3D**). [23,28].

PS-Mo expressed CX3CR1, implying chemotactic responses to CX3CL1 (fractalkine) (**Figure 3B**). PS-Mo migration in trans-well assays increased with increasing doses of CX3CL1 in the lower compartment of the chamber (**Figure 3C**). This phenomenon was not due to chemokinesis, but chemotaxis, because CX3CL1 in the top compartment could not induce PS-Mo migration into the lower compartment of the chamber. [24] We next compared the antigen uptake ability of PS-Mo, PS-imDCs, and PS-mDCs by incubating them with Ovalbumin Alexa fluor 488 Conjugate. [26] PS-Mo had the highest ability to take up antigen and as DCs matured they lost their ability to endocytose antigens (**Figure 3D**).

Functional Assays for DCs Derived from ESCs/iPSCs

For evaluating functions of PS-DCs, we first confirmed that patterns of expression of cell surface markers on PS-imDCs/mDCs were comparable to those on primary dendritic cells (**Figure 4A, Figure S4A**). When stimulated with LPS and TNFα, PS-DCs also produced almost comparable amounts of pro-inflammatory and anti-inflammatory cytokines (**Figure 4B, Figure S4B**).

To test the ability of PS-DCs to activate naïve T cells, we next co-cultured allogeneic naïve T cells with PS-DCs and PS-Mo. As shown in Figure 4C, PS-mDCs had the most potent capacity to stimulate allogeneic T cell proliferation and this dose-response relationship was comparable to that observed with PB-DCs (Figure S4C).

Functional Assays for Macrophages Derived from ESCs/iPSCs

Using this technique, we obtained morphologically typical macrophage-like cells that adhered firmly to the culture dish. To test whether these PS-MPs possessed functional plasticity like primary macrophages, we tried to polarize them into M1 or M2 state by treating them with IFNγ or IL-4, respectively. PS-MPs exhibited typical surface markers that were characteristic of primary M1 or M2 macrophages (**Figure 5A, Figure S5A**). The M1 cytokine pattern is typically IL-12^{high} and IL-10^{low}, whereas the M2 pattern is IL-12^{low} and IL-10^{high}. [5] Pluripotent cell-derived M1 and M2 macrophages (PS-M1/M2) also exhibited cytokine profiles that were comparable to those generated from primary monocytes (**Figure 5B, Figure S5B**).

Discussion

We have established a novel differentiation system for monocytic cells from human ES and iPS cells. Since macrophages and dendritic cells are usually obtained *in vitro* from monocytes, the most important point of the evaluation is to establish whether monocytes differentiated from ESCs/iPSCs are functionally comparable to primary monocytes. In several functional assays, PS-Mo indeed proved to be comparable to primary monocytes, and importantly, PS-DCs and PC-MPs from PS-Mo were also functionally comparable to their primary counterparts.

Although complete M1/M2 macrophage polarization still requires aserum-containing medium, the present results prove that the current method can precisely manipulate macrophages that have the potential to differentiate into M1/M2 macrophages. The cytokine profiles of PS-M1/M2 were also comparable to those of primary M1/M2 macrophages. The expression patterns of surface markers in PS-DCs after LPS stimulation and of PS-MPs after M1/M2 polarization were almost identical to those of DCs/MP derived from primary monocytes. However, the level of IL-10 in PS-DCs after stimulation was higher than that in primary DCs and the expression levels of HLA-DR in PS-DCs/MP were low in comparison with those in DCs/MP derived from primary monocytes. Therefore, further improvement of culture conditions such as the use of a modified medium and cytokine cocktail will be needed.

Several embryonic body methods and feeder cell co-culture methods for PS-DCs/MP differentiation have already been reported. [7,27,29–30] These methods show relatively poor-reproducibility because of the use of xenogeneic feeder cells and/or serum. In an earlier report which describes a protocol that can derive macrophages and dendritic cells from human iPSCs in feeder- and serum-free manner, [7] the authors did not fully characterize the monocytes and noted that PS-DCs/MP were generated only from two of the five iPSC clones tested. The current culture system simply propagated progenitor cells in 2-dimensional cultures without passage or sorting, and floating PS-Mo and PS-DCs/MP could be obtained repetitively from all five ESC/iPSC clones tested (**Figure S2 and S6**). These monocytic cells derived from disease- or patient- specific iPSC would be useful tools for the examination of disease pathologies and for drug discovery in immunological disorders such as autoimmune diseases, immunodeficiencies and autoinflammatory syndromes. However, even in our protocol, there are subtle clonal variations of timing of differentiation such as the day of step 3 to 4 switching which is determined by the emergence of CD43^{+}CD45^{+} cells (day 13–15, data not shown). Fine adjustment of the protocol for each ESC/iPSC clone seemed to further improve the yield of monocytes.

iPSC technology is overcoming immunological and ethical concerns in regenerative medicine using human pluripotent cells. Furthermore, a number of disease-associated iPSCs generated from patients with immunological disorders have been reported. [15,31–34] Because patient- or disease-specific iPS cells will be an important resource for unraveling human immunological disorders, a robust and simple hematopoietic differentiation system that can reliably mimic in vivo hematopoiesis is necessary for this purpose. Our simple and robust protocol to produce monocytic cells is therefore expected to be useful for regenerative medicine and studies of immunological disorders.

Supporting Information

Figure S1 Image of floating hematopoietic cells derived from iPS cells Phase contrast image of floating hematopoietic cells derived from iPS-201B7 at day 21 (step 4).
(PDF)

Figure S2 Phenotype analysis and gene expression pattern of monocytic lineage cells derived from 3 additional pluripotent stem cell lines. (A) The percentage of CD14+ cells within the total floating cells derived from 3 iPSC clones (253G4, CIRA188Ai-W2, and CB-A11) was evaluated from day 13 to day 28. (B) RT-PCR analysis of monocytic lineage cells derived from 253G4, CIRA188Ai-W2, and CB-A11 clones for expression of monocytic lineage marker genes (c-MAF, TLR4, and CCL17). Peripheral blood monocytes and peripheral blood monocyte-derived mature DCs were used as positive controls.
(PDF)

Figure S3 Characteristics of primary monocytes and macrophages. (A) Phase contrast image and (B) flow cytometric analysis of macrophages derived from primary monocytes. (C) The levels of IL-6 and TNF-α in supernatants of primary monocyte culture medium 4 hours after LPS stimulation. (D) The levels of IL-1β were measured 4 hours after LPS stimulation with/without an additional 30-minute ATP stimulation.
(PDF)

Figure S4 Characteristics and functional assays of dendritic cells derived from primary monocytes. (A) Flow cytometric analysis of immature/mature DCs derived from primary monocytes. (B) The levels of IL-10 and TNF-α in supernatants of culture medium with primary-DCs 24 hours after LPS stimulation. (C) The proliferation of allogeneic naïve T cells (1×105 cells per well) co-cultured with 40 Gy-irradiated stimulator cells for 3 days was evaluated. The proliferation of naïve T cells in the last 16 hours was measured by 3H-thymidine uptake.
(PDF)

Figure S5 Characteristics and functional assays of M1/M2 macrophages derived from primary monocytes. (A) Flow cytometric analysis of M1/M2 macrophages derived from primary monocytes. (B) The levels of IL-12p70 and IL-10 in supernatants of culture medium with M1/M2 macrophages derived from primary monocytes 24 hours after LPS stimulation.
(PDF)

Figure S6 Replication assays for 3 additional pluripotent stem cell lines. (A) Phase contrast image (left) and May-Giemsa staining (right) of mature DCs derived from iPSC clones. (B) Phase contrast image of macrophages derived from iPSC clones. (C) Flow cytometric analysis of immature/mature DCs and macrophages derived from iPSC clones.
(PDF)

Table S1 Primers for RT-PCR.
(PDF)

Acknowledgments

We are grateful to Y. Sasaki, Y. Jindai, K. Kobayashi, M. Yamane, and S. Nakamura for technical assistance. We would also like to thank N. Takasu and Y. Takao for administrative assistance.

Author Contributions

iPSC establishment: MDY IA. Conceived and designed the experiments: MDY AN HG TH TN MKS. Performed the experiments: MDY ST SN YM TT JI FHO. Analyzed the data: MDY AN TY KO TN MKS. Wrote the paper: MDY AN TY MKS.

References

1. Auffray C, Sieweke MH, Geissmann F (2009) Blood monocytes: development, heterogeneity, and relationship with dendritic cells. Annu Rev Immunol 27: 669–692.
2. Mosser DM, Edwards JP (2008) Exploring the full spectrum of macrophage activation. Nat Rev Immunol 8: 958–969.
3. Geissmann F, Manz MG, Jung S, Sieweke MH, Merad M, et al. (2010) Development of monocytes, macrophages, and dendritic cells. Science 327: 656–661.
4. Ingersoll MA, Platt AM, Potteaux S, Randolph GJ (2011) Monocyte trafficking in acute and chronic inflammation. Trends Immunol 32: 470–477.
5. Mantovani A, Sozzani S, Locati M, Allavena P, Sica A (2002) Macrophage polarization: tumor-associated macrophages as a paradigm for polarized M2 mononuclear phagocytes. Trends Immunol 23: 549–555.
6. Boudreau JE, Bonehill A, Thielemans K, Wan Y (2011) Engineering dendritic cells to enhance cancer immunotherapy. Mol Ther 19: 841–853.
7. Senju S, Haruta M, Matsumura K, Matsunaga Y, Fukushima S, et al. (2011) Generation of dendritic cells and macrophages from human induced pluripotent stem cells aiming at cell therapy. Gene Ther 18: 874–883.
8. Collin M, Bigley V, Haniffa M, Hambleton S (2011) Human dendritic cell deficiency: the missing ID? Nat Rev Immunol 11: 575–583.
9. Thomson JA, Itskovitz-Eldor J, Shapiro SS, Waknitz MA, Swiergiel JJ, et al. (1998) Embryonic stem cell lines derived from human blastocysts. Science 282: 1145–1147.
10. Takahashi K, Tanabe K, Ohnuki M, Narita M, Ichisaka T, et al. (2007) Induction of pluripotent stem cells from adult human fibroblasts by defined factors. Cell 131: 861–872.
11. Yamanaka S (2007) Strategies and new developments in the generation of patient-specific pluripotent stem cells. Cell Stem Cell 1: 39–49.
12. Orlovskaya I, Schraufstatter I, Loring J, Khaldoyanidi S (2008) Hematopoietic differentiation of embryonic stem cells. Methods 45: 159–167.
13. Royer PJ, Tanguy-Royer S, Ebstein F, Sapede C, Simon T, et al. (2006) Culture medium and protein supplementation in the generation and maturation of dendritic cells. Scand J Immunol 63: 401–409.
14. Suemori H, Yasuchika K, Hasegawa K, Fujioka T, Tsuneyoshi N, et al. (2006) Efficient establishment of human embryonic stem cell lines and long-term maintenance with stable karyotype by enzymatic bulk passage. Biochem Biophys Res Commun 345: 926–932.
15. Tanaka T, Takahashi K, Yamane M, Tomida S, Nakamura S, et al. (2012) Induced pluripotent stem cells from CINCA syndrome patients as a model for dissecting somatic mosaicism and drug discovery. Blood.
16. Okita K, Matsumura Y, Sato Y, Okada A, Morizane A, et al. (2011) A more efficient method to generate integration-free human iPS cells. Nat Methods 8: 409–412.
17. Niwa A, Heike T, Umeda K, Oshima K, Kato I, et al. (2011) A novel serum-free monolayer culture for orderly hematopoietic differentiation of human pluripotent cells via mesodermal progenitors. PLoS One 6: e22261.
18. Pick M, Azzola L, Mossman A, Stanley EG, Elefanty AG (2007) Differentiation of human embryonic stem cells in serum-free medium reveals distinct roles for bone morphogenetic protein 4, vascular endothelial growth factor, stem cell factor, and fibroblast growth factor 2 in hematopoiesis. Stem Cells 25: 2206–2214.
19. Umeda K, Heike T, Yoshimoto M, Shiota M, Suemori H, et al. (2004) Development of primitive and definitive hematopoiesis from nonhuman primate embryonic stem cells in vitro. Development 131: 1869–1879.
20. Yu P, Pan G, Yu J, Thomson JA (2011) FGF2 sustains NANOG and switches the outcome of BMP4-induced human embryonic stem cell differentiation. Cell Stem Cell 8: 326–334.
21. Friedman AD (2007) Transcriptional control of granulocyte and monocyte development. Oncogene 26: 6816–6828.
22. Zhong W, Fei M, Zhu Y, Zhang X (2009) Transcriptional profiles during the differentiation and maturation of monocyte-derived dendritic cells, analyzed using focused microarrays. Cell Mol Biol Lett 14: 587–608.
23. Mariathasan S, Weiss DS, Newton K, McBride J, O'Rourke K, et al. (2006) Cryopyrin activates the inflammasome in response to toxins and ATP. Nature 440: 228–232.
24. Gevrey JC, Isaac BM, Cox D (2005) Syk is required for monocyte/macrophage chemotaxis to CX3CL1 (Fractalkine). J Immunol 175: 3737–3745.
25. Morishima T, Watanabe K, Niwa A, Fujino H, Matsubara H, et al. (2011) Neutrophil differentiation from human-induced pluripotent stem cells. J Cell Physiol 226: 1283–1291.
26. Li GB, Lu GX (2010) Adherent cells in granulocyte-macrophage colony-stimulating factor-induced bone marrow-derived dendritic cell culture system are qualified dendritic cells. Cell Immunol 264: 4–6.
27. Choi KD, Vodyanik MA, Slukvin II (2009) Generation of mature human myelomonocytic cells through expansion and differentiation of pluripotent stem cell-derived lin-CD34+CD43+CD45+ progenitors. J Clin Invest 119: 2818–2829.
28. Hogquist KA, Nett MA, Unanue ER, Chaplin DD (1991) Interleukin 1 is processed and released during apoptosis. Proc Natl Acad Sci U S A 88: 8485–8489.
29. Su Z, Frye C, Bae KM, Kelley V, Vieweg J (2008) Differentiation of human embryonic stem cells into immunostimulatory dendritic cells under feeder-free culture conditions. Clin Cancer Res 14: 6207–6217.
30. Tseng SY, Nishimoto KP, Silk KM, Majumdar AS, Dawes GN, et al. (2009) Generation of immunogenic dendritic cells from human embryonic stem cells without serum and feeder cells. Regen Med 4: 513–526.
31. Jiang Y, Cowley SA, Siler U, Melguizo D, Tilgner K, et al. (2012) Derivation and functional analysis of patient-specific induced pluripotent stem cells as an in vitro model of chronic granulomatous disease. Stem Cells 30: 599–611.
32. Park IH, Arora N, Huo H, Maherali N, Ahfeldt T, et al. (2008) Disease-specific induced pluripotent stem cells. Cell 134: 877–886.
33. Pessach IM, Ordovas-Montanes J, Zhang SY, Casanova JL, Giliani S, et al. (2011) Induced pluripotent stem cells: a novel frontier in the study of human primary immunodeficiencies. J Allergy Clin Immunol 127: 1400–1407 e1404.
34. Zou J, Sweeney CL, Chou BK, Choi U, Pan J, et al. (2011) Oxidase-deficient neutrophils from X-linked chronic granulomatous disease iPS cells: functional correction by zinc finger nuclease-mediated safe harbor targeting. Blood 117: 5561–5572.

Genetic correction of *HAX1* in induced pluripotent stem cells from a patient with severe congenital neutropenia improves defective granulopoiesis

Tatsuya Morishima,[1] Ken-ichiro Watanabe,[1] Akira Niwa,[2] Hideyo Hirai,[3] Satoshi Saida,[1] Takayuki Tanaka,[2] Itaru Kato,[1] Katsutsugu Umeda,[1] Hidefumi Hiramatsu,[1] Megumu K. Saito,[2] Kousaku Matsubara,[4] Souichi Adachi,[5] Masao Kobayashi,[6] Tatsutoshi Nakahata,[2] and Toshio Heike[1]

[1]Department of Pediatrics, Graduate School of Medicine, Kyoto University, Kyoto; [2]Department of Clinical Application, Center for iPS Cell Research and Application, Kyoto University, Kyoto; [3]Department of Transfusion Medicine and Cell Therapy, Kyoto University Hospital, Kyoto; [4]Department of Pediatrics, Nishi-Kobe Medical Center, Kobe; [5]Human Health Sciences, Graduate School of Medicine, Kyoto University, Kyoto; and [6]Department of Pediatrics, Hiroshima University Graduate School of Biomedical Sciences, Hiroshima, Japan

ABSTRACT

HAX1 was identified as the gene responsible for the autosomal recessive type of severe congenital neutropenia. However, the connection between mutations in the *HAX1* gene and defective granulopoiesis in this disease has remained unclear, mainly due to the lack of a useful experimental model for this disease. In this study, we generated induced pluripotent stem cell lines from a patient presenting for severe congenital neutropenia with *HAX1* gene deficiency, and analyzed their *in vitro* neutrophil differentiation potential by using a novel serum- and feeder-free directed differentiation culture system. Cytostaining and flow cytometric analyses of myeloid cells differentiated from patient-derived induced pluripotent stem cells showed arrest at the myeloid progenitor stage and apoptotic predisposition, both of which replicated abnormal granulopoiesis. Moreover, lentiviral transduction of the *HAX1* cDNA into patient-derived induced pluripotent stem cells reversed disease-related abnormal granulopoiesis. This *in vitro* neutrophil differentiation system, which uses patient-derived induced pluripotent stem cells for disease investigation, may serve as a novel experimental model and a platform for high-throughput screening of drugs for various congenital neutrophil disorders in the future.

Introduction

Severe congenital neutropenia (SCN) is a rare myelopoietic disorder resulting in recurrent life-threatening infections due to a lack of mature neutrophils,[1] and individuals with SCN present for myeloid hypoplasia with an arrest of myelopoiesis at the promyelocyte/myelocyte stage.[1,2] SCN is actually a multigene syndrome that can be caused by inherited mutations in several genes. For instance, approximately 60% of SCN patients are known to carry autosomal dominant mutations in the *ELANE* gene, which encodes neutrophil elastase (NE).[3] An autosomal recessive type of SCN was first described by Kostmann in 1956,[4] and defined as Kostmann disease. Although the gene responsible for this classical type of SCN remained unknown for more than 50 years, Klein *et al.* identified mutations in *HAX1* to be responsible for this type of SCN in 2007.[5] HAX1 localizes predominantly to mitochondria, where it controls inner mitochondrial membrane potential ($\Delta\psi_m$) and apoptosis.[6,7] Although an increase in apoptosis in mature neutrophils was presumed to cause neutropenia in HAX1 gene deficiency,[5] the connection between *HAX1* gene mutations and defective granulopoiesis in SCN has remained unclear.

To control infections, SCN patients are generally treated with granulocyte colony-stimulating factor (G-CSF); however, long-term G-CSF therapy associates with an increased risk of myelodysplastic syndrome and acute myeloid leukemia (MDS/AML).[8,9] Although hematopoietic stem cell transplantations are available as the only curative therapy for this disease, they can result in various complications and mortality.[4]

Many murine models of human congenital and acquired diseases are invaluable for disease investigation as well as for novel drug discoveries. However, their use in a research setting can be limited if they fail to mimic strictly the phenotype of the human disease in question. For instance, the *Hax1* knock-out mouse is characterized by lymphocyte loss and neuronal apoptosis, but not neutropenia.[10] Thus, it is not a suitable experimental model for SCN. Induced pluripotent stem (iPS) cells are reprogrammed somatic cells with embryonic stem (ES) cell-like characteristics produced by the introduction of specific transcription factors,[11,16] and they may substitute murine models of human disease. It is believed that iPS cell technology, which generates disease-specific pluripotent stem cells in combination with directed cell differentiation, will contribute enormously to patient-oriented research, including disease pathophysiology, drug screening, cell transplantation, and gene therapy.

In vitro neutrophil differentiation systems, which can reproduce the differentiation of myeloid progenitor cells to mature neutrophils, are needed to understand the pathogenesis of SCN better. Recently, we established a neutrophil differentia-

 doi:10.3324/haematol.2013.083873
The online version of this article has a Supplementary Appendix.
Manuscript received on January 9, 2013. Manuscript accepted on August 20, 2013.
Correspondence: heike@kuhp.kyoto-u.ac.jp

tion system from human iPS cells[17] as well as a serum- and feeder-free monolayer hematopoietic culture system from human ES and iPS cells.[18] In this study, we generate iPS cell lines from an SCN patient with *HAX1* gene deficiency and differentiate them into neutrophils *in vitro*. Furthermore, we corrected for the *HAX1* gene deficiency in HAX1-iPS cells by lentiviral transduction with *HAX1* cDNA and analyzed the neutrophil differentiation potential of these cells. Thus, this *in vitro* neutrophil differentiation system from patient-derived iPS cells may be a useful model for future studies in SCN patients with *HAX1* gene deficiency.

Methods

Human iPS cell generation

Skin biopsy specimens were obtained from an 11-year old male SCN patient with *HAX1* gene deficiency.[19] This study was approved by the Ethics Committee of Kyoto University, and informed consent was obtained from the patient's guardians in accordance with the Declaration of Helsinki. Fibroblasts were expanded in DMEM (Nacalai Tesque, Inc., Kyoto, Japan) containing 10% FBS (vol/vol, Invitrogen, Carlsbad, CA, USA) and 0.5% penicillin and streptomycin (wt/vol, Invitrogen). Generation of iPS cells was performed as described previously.[12] In brief, we introduced *OCT3/4, SOX2, KLF4*, and *cMYC* using ecotropic retroviral transduction into patient's fibroblasts expressing mouse *Slc7a1*. Six days after transduction, cells were harvested and re-plated onto mitotically inactive SNL feeder cells. On the following day, DMEM was replaced with primate ES cell medium (ReproCELL, Kanagawa, Japan) supplemented with basic fibroblast growth factor (5 ng/mL, R&D Systems, Minneapolis, MN, USA). Three weeks later, individual colonies were isolated and expanded.

Maintenance of cells

Control ES (KhES-1) and control iPS (253G4 and 201B6) cells were kindly provided by Drs. Norio Nakatsuji and Shinya Yamanaka (Kyoto University, Kyoto, Japan), respectively. These human ES and iPS cell lines were maintained on mitomycin-C (Kyowa Hakko Kirin, Tokyo, Japan)-treated SNL feeder cells as described previously[17] and subcultured onto new SNL feeder cells every seven days.

Flow cytometric analysis

Cells were stained with antibodies as reported previously.[17] Samples were analyzed using an LSR flow cytometer and Cell Quest software (Becton-Dickinson).

Neutrophil differentiation of iPS cells

In a previous study, we established a serum and feeder-free monolayer hematopoietic culture system from human ES and iPS cells.[18] In this study, we modified this culture system to direct neutrophil differentiation. iPS cell colonies were cultured on growth factor-reduced Matrigel (Becton-Dickinson)-coated cell culture dishes in Stemline II hematopoietic stem cell expansion medium (Sigma-Aldrich, St. Louis, MO, USA) containing the insulin-transferrin-selenium (ITS) supplement (Invitrogen) and cytokines. iPS cells were treated with cytokines as follows: bone morphogenetic protein (BMP) 4 (20 ng/mL, R&D Systems) was added for four days and then replaced with vascular endothelial growth factor (VEGF) 165 (40 ng/mL, R&D Systems) on Day 4. On Day 6, VEGF 165 was replaced with a combination of stem cell factor (SCF, 50 ng/mL, R&D Systems), interleukin (IL)-3 (50 ng/mL, R&D Systems), thrombopoietin (TPO, 5 ng/mL, kindly provided by Kyowa Hakko Kirin), and G-CSF (50 ng/mL, also kindly provided by Kyowa Hakko Kirin). Thereafter, medium was replaced every five days.

Dead cell removal and CD45$^+$ leukocyte separation

Floating cells were collected, followed by the removal of dead cells and cellular debris with the Dead Cell Removal kit (Miltenyi Biotec, Bergisch Gladbach, Germany). CD45$^+$ cells were then separated using human CD45 microbeads (Miltenyi Biotec). Cell separation procedures were performed using the autoMACS Pro Separator (Miltenyi Biotec).

Statistical analysis

Statistical analysis was carried out using Student's t-test. $P<0.05$ was considered statistically significant.

Results

Generation of iPS cell lines from an SCN patient with HAX1 gene deficiency

To generate patient-derived iPS cell lines, dermal fibroblasts were obtained from a male SCN patient with a homozygous 256C-to-T transition resulting in an R86X mutation in the *HAX1* gene.[19] These fibroblasts were reprogrammed to iPS cells after transduction with retroviral vectors encoding *OCT3/4, SOX2, KLF4* and *cMYC*,[12] and a total of 11 iPS cell clones were obtained. From these, we randomly selected three clones for propagation and subsequent analyses. One of these clones (HAX1 4F5) was generated with four factors (*OCT3/4, SOX2, KLF4*, and *cMYC*); the remaining clones (HAX1 3F3 and 3F5) were generated with three factors (*OCT3/4, SOX2*, and *KLF4*).[12]

All of these patient-derived iPS cell clones showed a characteristic human ES cell-like morphology (Figure 1A), and they propagated for serial passages in human ES cell maintenance culture medium. Quantitative PCR analysis showed the expression of *NANOG*, a pluripotent marker gene, to be comparable to that of control ES (KhES-1) and iPS (253G4 and 201B6) cells (Figure 1B). Surface marker analysis indicated that they were also positive for SSEA4, a human ES and iPS cell marker (Figure 1C). DNA sequencing analysis verified an identical mutation in the *HAX1* gene in all established iPS cell clones (Figure 1D). The pluripotency of all iPS cell clones was confirmed by the presence of cell derivatives representing all three germ layers by teratoma formation after subcutaneous injection of undifferentiated iPS cells into immunocompromised NOD/SCID/γc^{null} mice (Figure 1E).

To validate the authenticity of iPS cells further, we investigated the expression of the four genes that were used for iPS cell generation. The expression level of all endogenous genes was comparable to control ES and iPS cells. On the other hand, transgene expression was largely undetectable in patient-derived iPS cell clones (*Online Supplementary Figure S1A*). Chromosomal analysis revealed that all patient-derived iPS cell clones maintained a normal karyotype (*Online Supplementary Figure S1B*). Genetic identity was shown by short tandem repeat analysis (*Online Supplementary Figure S1C*).

Taken collectively, these results indicate that iPS cell clones were comprised of good quality iPS cells derived from the somatic cells of an SCN patient with *HAX1* gene deficiency (HAX1-iPS cells).

Maturation arrest at the progenitor level in neutrophil differentiation from HAX1-iPS cells

The paucity of mature neutrophils in the peripheral blood and a maturation arrest at the promyelocyte/myelocyte stage in the bone marrow are characteristic laboratory findings presented in the SCN patients with *HAX1* gene deficiency. To investigate whether our patient-derived iPS cell model accurately replicated this disease phenotype, we assessed neutrophil differentiation from HAX1-iPS cells by using a serum- and feeder-free monolayer culture system[18] with minor modifications (Online *Supplementary Figure S2*).

In this system, we cultured iPS cell colonies on Matrigel-coated dishes in serum-free medium supplemented with several cytokines and obtained hematopoietic cells as floating cells on approximately Day 26 of differentiation. May-Giemsa staining of floating live CD45$^+$ cells derived from normal iPS cells showed that approximately 40% were mature neutrophils (Figure 2A and B). The remaining cells consisted of immature myeloid cells as well as a small number of macrophages. Cells of other lineages such as erythroid or lymphoid cells were not observed. On the other hand, HAX1-iPS cell-derived blood cells contained only approximately 10% mature neutrophils and approxi-

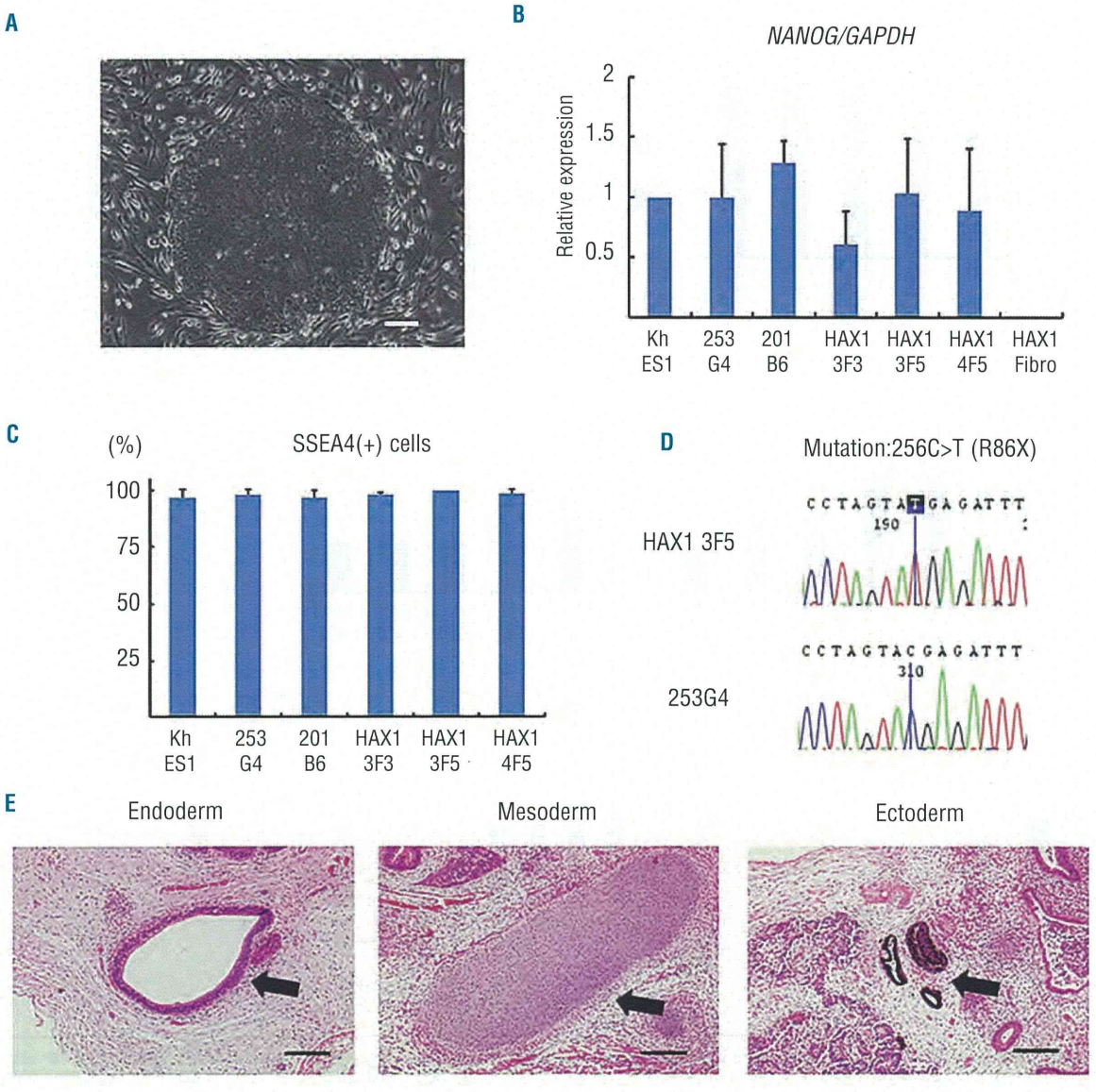

Figure 1. Generation of iPS cell lines from an SCN patient with *HAX1* gene deficiency. (A) Human ES cell-like morphology of HAX1-iPS cells. Scale bar: 200 μm. (B) *NANOG* expression in HAX1-iPS cells, control iPS cells (253G4 and 201B6), and patient-derived fibroblasts (HAX1 Fibro) compared to control ES cells (KhES1). *GAPDH* was used as an internal control (n = 3; bars represent SDs). (C) SSEA-4 expression analysis using flow cytometry. Gated on TRA1-85$^+$DAPI$^-$ cells as viable human iPS (ES) cells (n = 3; bars represent SDs). (D) DNA sequencing analysis of the *HAX1* gene in iPS cells. HAX1-iPS cells showed 256C>T (R86X) mutation that was found in the patient. (E) Teratoma formation from HAX1-iPS cells in the NOD/SCID/γc^{null} (NOG) mouse. Arrows indicate the following; Endoderm: respiratory epithelium; Mesoderm: cartilage; Ectoderm: pigmented epithelium. Scale bars: 200 μm. (A, D-E) Representative data (HAX1 3F5) are shown.

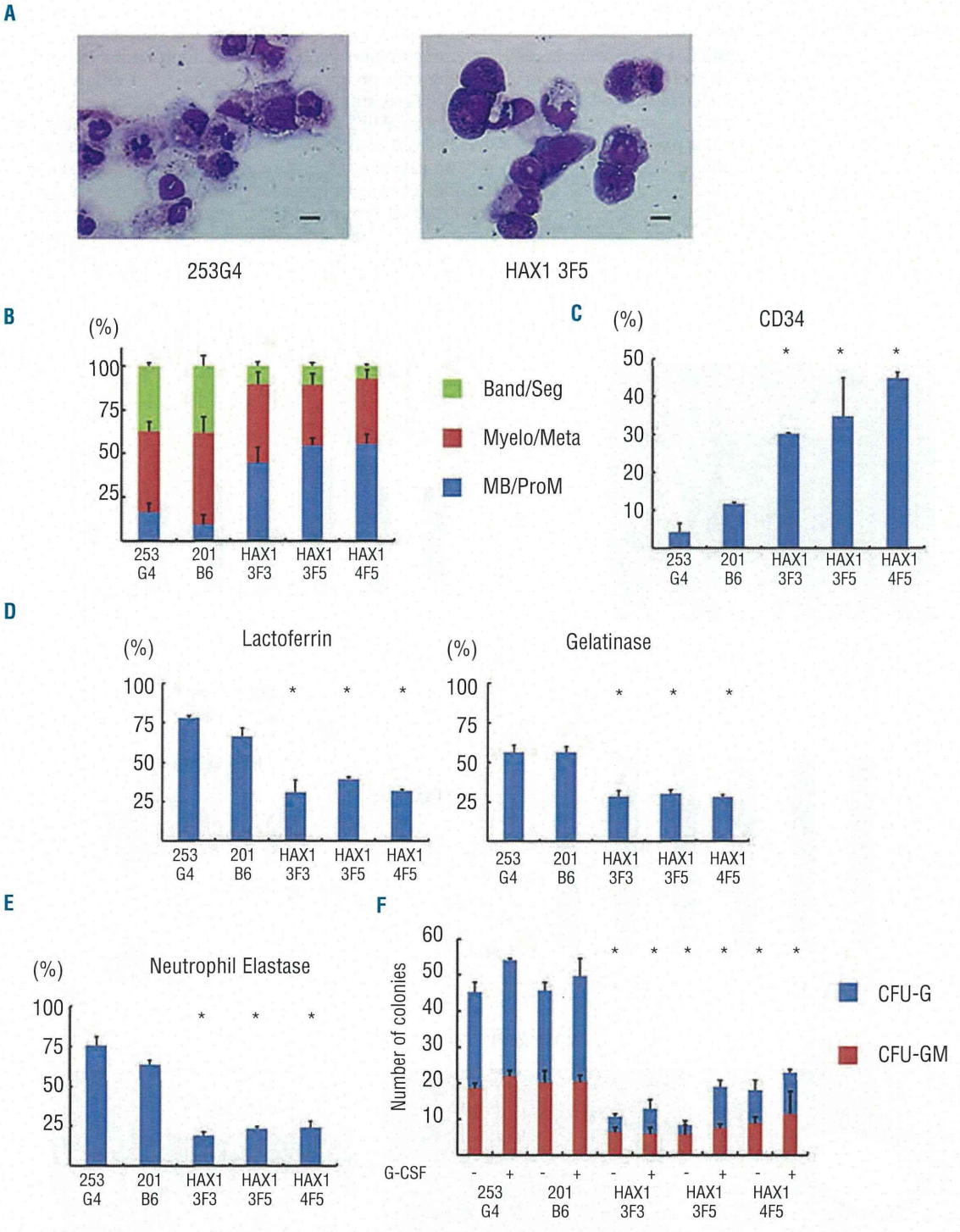

Figure 2. Maturation arrest at the progenitor level in neutrophil differentiation from HAX1-iPS cells. (A) May-Giemsa staining of CD45$^+$ cells derived from normal (253G4) and HAX1-iPS (HAX1 3F5) cells. Scale bars: 10 μm. (B) Morphological classification of CD45$^+$ cells derived from iPS cells. Cells were classified into three groups: myeloblast and promyelocyte (MB/ProM), myelocyte and metamyelocyte (Myelo/Meta), and band and segmented neutrophils (Band/Seg) (n = 3; bars represent SDs). (C) Flow cytometric analysis of CD45$^+$ cells derived from iPS cells. Cells gated on human CD45$^+$ DAPI$^-$ were analyzed (n = 3; bars represent SDs; *P<0.05 compared to control iPS cells). (D) Immunocytochemical analysis of CD45$^+$ cells derived from iPS cells (n = 3; bars represent SDs; *P<0.05 compared to control iPS cells). (E) NE staining of CD45$^+$ cells derived from iPS cells (n = 3; bars represent SDs; *P<0.05 compared to control iPS cells). (F) Colony-forming assay of cells derived from iPS cells. On Day 16, living adherent cells were collected and cultured in methylcellulose medium (see *Online Supplementary Appendix*). The number of colonies generated from 1×10^4 cells is indicated (n = 3; bars represent SD; *P<0.05 compared to control iPS cells). (A–E) Live CD45$^+$ cells derived from normal and HAX1-iPS cells on Day 26 of neutrophil differentiation were analyzed. Dead cells and CD45$^-$ cells were depleted using an autoMACS Pro separator (see *Methods*).

mately 50% immature myeloid cells, including myeloblasts and promyelocytes (Figure 2A and B). Flow cytometric analysis revealed that the percentage of CD34$^+$ cells within HAX1-iPS cell-derived blood cells was significantly higher than in normal iPS cell-derived blood cells (Figure 2C), which also showed that the percentage of phenotypically immature myeloid cells was higher in HAX1-iPS cell-derived blood cells than in normal iPS cell-derived blood cells.

Immunocytochemical analysis for lactoferrin and gelatinase, which are constitutive proteins of neutrophil specific granules observed in mature neutrophils, showed that the proportion of these granule-positive cells was significantly lower in HAX1-iPS cell-derived blood cells than in normal iPS cell-derived blood cells (Figure 2D). NE is a protease stored in primary granules of neutrophilic granulocytes that are formed at the promyelocytic phase of granulocyte differentiation. *ELANE* mRNA expression in myeloid progenitors and the protein level of NE in plasma are markedly reduced in SCN patients with mutations in *ELANE* or *HAX1*.[20] Consistent with this, the proportion of NE-positive cells was significantly lower in blood cells derived from HAX1-iPS cells than in those derived from normal iPS cells (Figure 2E). Thus, the level of functionally mature neutrophils decreased during *in vitro* granulopoietic differentiation of HAX1-iPS cells.

Next, we analyzed the colony-forming potential of HAX1-iPS cell-derived myeloprogenitor cells. Significantly fewer colonies, which were classified as granulocyte-macrophage (GM) or granulocyte (G) colony-forming units (CFU), were derived from HAX1-iPS cells than from control iPS cells. Furthermore, the colonies derived from HAX1-iPS cells were predominantly CFU-GM (Figure 2F). Thus, maturation arrest occurred at the clonogenic progenitor stage during *in vitro* neutrophil differentiation of HAX1-iPS cells.

SCN is characterized by severe neutropenia with very low absolute neutrophil counts in peripheral blood, and many SCN patients respond to G-CSF treatment.[1,2] In colony-forming assays using bone marrow cells of SCN patients, primitive myeloid progenitor cells have reduced responsiveness to hematopoietic cytokines including G-CSF.[21,22] Therefore, we next examined the response of HAX1-iPS cell-derived blood cells to G-CSF using a colony-forming assay. Although the number of colonies derived from HAX1-iPS cells slightly increased following the addition of G-CSF, it remained significantly lower than the number of colonies derived from control iPS cells in the absence of G-CSF (Figure 2F). These results indicate that the responsiveness of HAX1-iPS-derived blood cells to G-CSF was insufficient to restore the neutrophil count to a normal level and are consistent with the fact that the absolute neutrophil counts of SCN patients remain low following G-CSF therapy.[19,21]

Neutrophils derived from HAX1-iPS cells are predisposed to undergo apoptosis due to their reduced $\Delta\psi_m$

Previous studies have shown HAX1 to localize to mitochondria[6] and to mediate anti-apoptotic activity.[7] Interestingly, this apoptotic predisposition of neutrophils due to their reduced $\Delta\psi_m$ was observed in HAX1-deficient patients,[5] prompting us to examine apoptosis in HAX1-iPS cell-derived blood cells. Consistent with these reports, HAX1-iPS cell-derived blood cells showed a significantly higher percentage of Annexin V-positive cells than in control cells (Figure 3A). In addition, a mitochondrial membrane potential assay revealed that the percentage of cells with a low $\Delta\psi_m$ was significantly higher in HAX1-iPS cell-derived blood cells than in blood cells derived from control iPS cells (Figure 3B). By contrast, the percentage of cells with a low $\Delta\psi_m$ was similar in undifferentiated HAX1-iPS cells and undifferentiated control iPS cells (*Online Supplementary Figure S3*).

Thus, increased apoptosis due to reduced $\Delta\psi_m$ causes defective granulopoiesis during neutrophil differentiation from HAX1-iPS cells, similar to the process observed in SCN patients with *HAX1* gene deficiency.

Lentiviral transduction of HAX1 cDNA improves maturation arrest and apoptotic predisposition of HAX1-iPS cells

Because most *HAX1* gene mutations in SCN patients are nonsense mutations resulting in a premature stop codon and protein truncation,[23] loss of the HAX1 protein is believed to cause severe neutropenia. To uncover the pathophysiological hallmarks of this disease, we performed lentiviral transduction of *HAX1* cDNA into HAX1-iPS cells.

We constructed lentiviral vectors that expressed *HAX1* cDNA and EGFP as a marker gene (pCSII-EF-IEGFP; EGFP

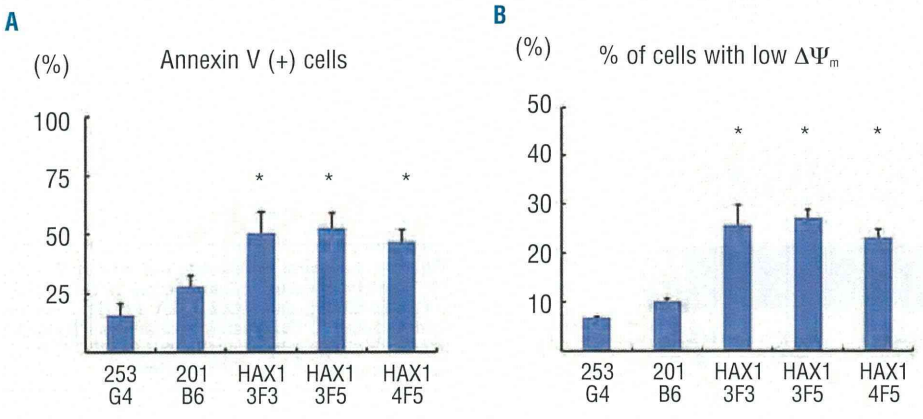

Figure 3. Neutrophils derived from HAX1-iPS cells are predisposed to undergo apoptosis due to their reduced $\Delta\psi$m. Annexin V assay (A) and mitochondrial membrane potential assay (B) of iPS cell-derived cells on Day 26 of neutrophil differentiation using flow cytometry. Cells gated on human CD45$^+$ were analyzed (n = 3; bars represent SDs; *P<0.05 to control iPS cells).

only, pCSII-EF-HAX1-IEGFP; HAX1 cDNA and EGFP) (Figure 4A). Efficient transduction of HAX1-iPS cells with these lentiviral vectors (HAX1 3F5+GFP; HAX1 3F5 transduced with pCSII-EF-IEGFP, HAX1 3F5+HAX1; HAX1 3F5 transduced with pCSII-EF-HAX1-IEGFP) was confirmed by a significant increase in HAX1 protein by Western blotting analysis (Figure 4B).

We then differentiated these lentiviral-transduced iPS cells into neutrophils, and examined whether defective granulopoiesis and apoptotic predisposition could be reversed. Morphologically, cells derived from HAX1 3F5+HAX1 showed a higher proportion of mature neutrophils than cells derived from HAX1 3F5+GFP and HAX1 3F5 (Figure 5A and B). Flow cytometric analysis revealed that the proportion of $CD34^+$ cells was significantly lower in the cells derived from HAX1 3F5+HAX1 than HAX1 3F5+GFP and HAX1 3F5 (Figure 5C). Immunocytochemical analysis for lactoferrin and gelatinase showed that the proportion of these granule-positive cells in generated blood cells was significantly higher in HAX 3F5+HAX1 than in HAX13F5+GFP and HAX1 3F5 (Figure 5D). These results indicated that *HAX1* cDNA increased the number of mature neutrophils in the neutrophil differentiation culture from HAX1-iPS cells *in vitro*. In addition, the percentage of NE-positive cells was significantly higher in cells derived from HAX1 3F5+HAX1 than in cells derived from HAX1 3F5+GFP and HAX1 3F5 (Figure 5E). Furthermore, the number of colonies derived from HAX1 3F5+HAX1 was comparable to the number derived from control cells (Figure 5F).

HAX1 3F5+HAX1-derived blood cells showed a significantly lower percentage of Annexin V-positive cells (Figure 6A) and a significantly lower percentage of cells with a low $\Delta\psi_m$ (Figure 6B) than HAX13F5+GFP and HAX1 3F5-derived blood cells. These results indicated that only *HAX1* cDNA transduction improved defective granulopoiesis and apoptotic predisposition due to low $\Delta\psi_m$ in the neutrophil differentiation culture from HAX1-iPS cells *in vitro*.

Discussion

Animal models and *in vitro* cultures consisting of cells derived from patients are often used to investigate disease pathophysiology and to develop novel therapies. Unfortunately, *Hax1* knock-out mice fail to reproduce abnormal granulopoiesis as observed in SCN patients.[10] Moreover, bone marrow cells are not an ideal experimental tool because it is difficult to obtain sufficient blood cells due to the invasiveness of the aspiration procedure. Moreover, the pathophysiological mechanisms occurring during early granulopoiesis are difficult to address in primary patient samples.

Our established culture system efficiently induced directed hematopoietic differentiation, which consisted of myeloid cells at different stages of development, from various control and patient-derived HAX1-iPS cell lines. Furthermore, this *in vitro* neutrophil differentiation system produced sufficient myeloid cells, which enabled us to perform various types of assays. In addition, flow cytom-

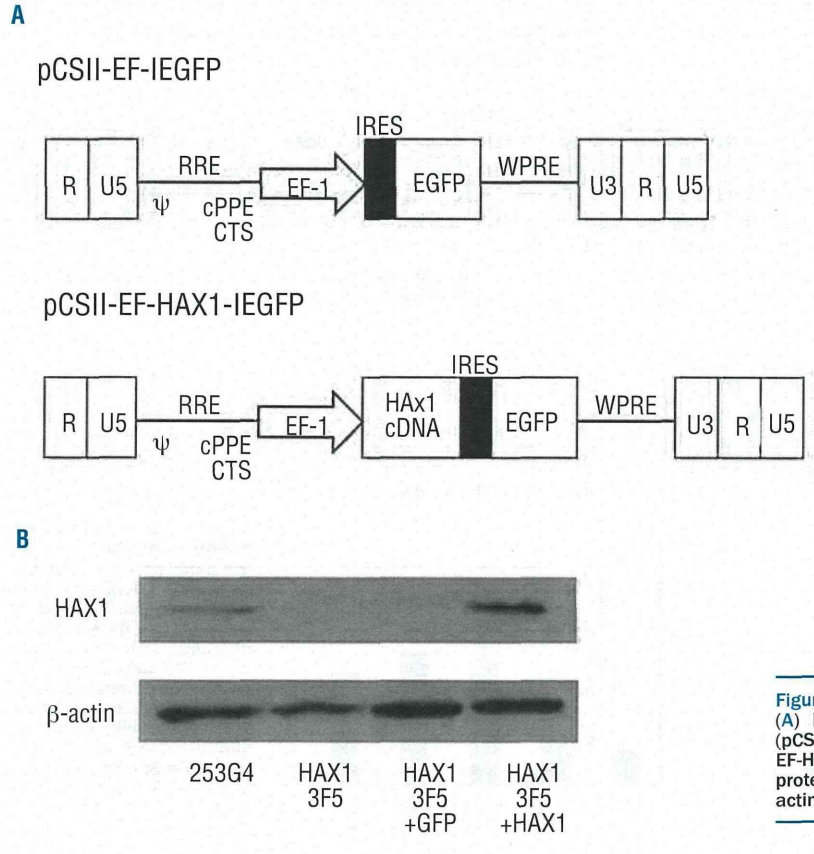

Figure 4. Lentiviral transduction of HAX1-iPS cells. (A) Lentiviral vector constructs with only EGFP (pCSII-EF-IEGFP), and *HAX1* cDNA and EGFP (pCSII-EF-HAX1-IEGFP). (B) Western blot analysis for HAX1 protein in lentivirally-transduced HAX1-iPS cells. β-actin was used as a loading control.

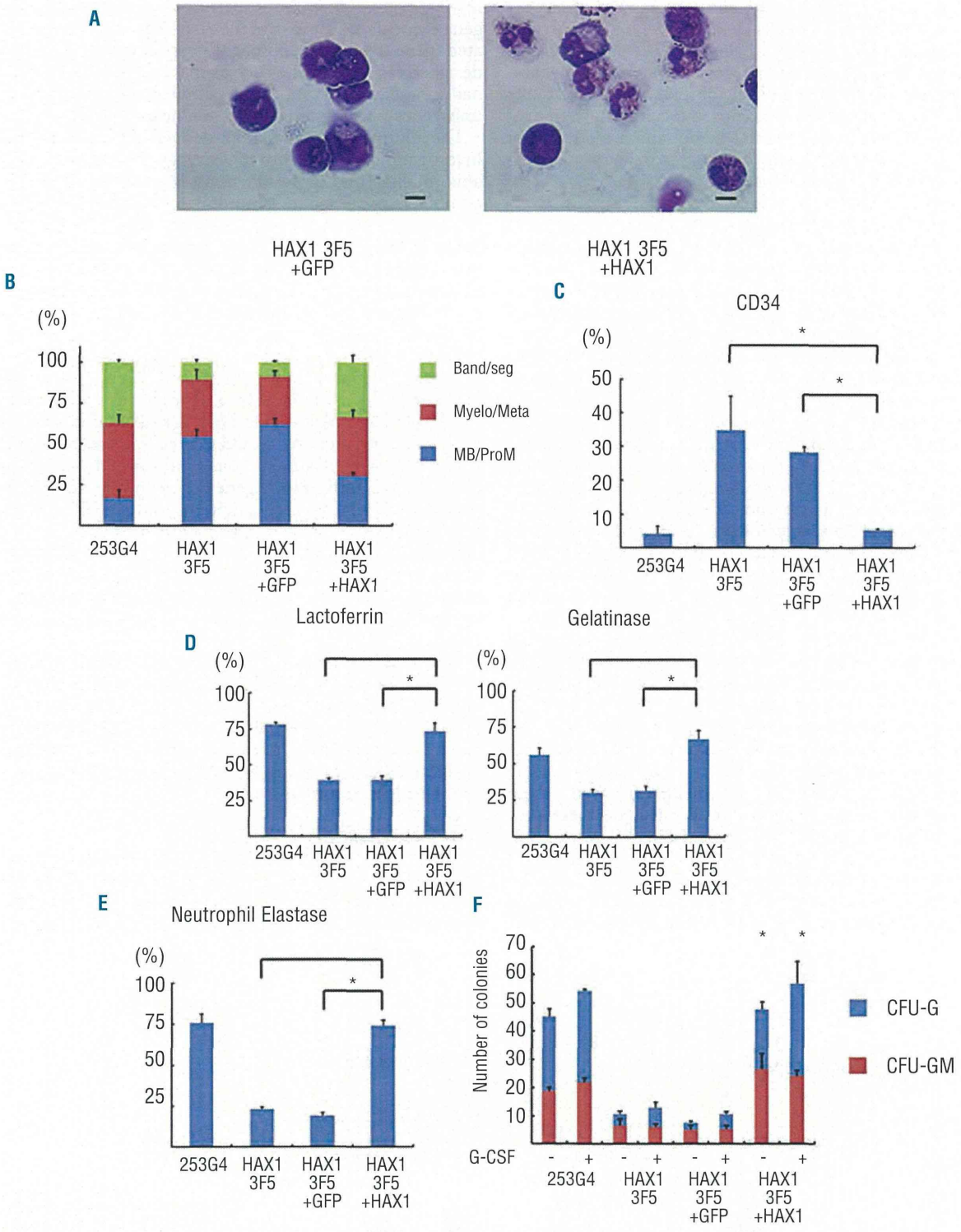

Figure 5. Lentiviral transduction of HAX1 cDNA improves maturation arrest of HAX1-iPS cells. (A) May-Giemsa staining of CD45$^+$ cells derived from HAX1 3F5+GFP and HAX1 3F5+HAX1 cells. Scale bars: 10 μm. (B) Morphological classification of CD45$^+$ cells derived from lentivirally-transduced iPS cells. (n = 3; bars represent SDs). (C) Flow cytometric analysis of CD45$^+$ cells derived from lentivirally-transduced iPS cells. Cells gated on GFP$^+$ human CD45$^+$ DAPI$^-$ were analyzed (n = 3; bars represent SDs; *P<0.05). (D) Immunocytochemical analysis of CD45$^+$ cells derived from lentivirally-transduced iPS cells (n = 3; bars represent SDs; *P<0.05). (E) NE staining of CD45$^+$ cells derived from lentivirally-transduced iPS cells (n = 3; bars represent SDs; *P<0.05). (F) Colony-forming assay of lentivirally-transduced cells derived from iPS cells. The number of colonies derived from 1×10^4 cells is indicated (n = 3; bars represent SD; *P<0.05 compared to HAX1 3F5 and HAX1 3F5+GFP). (A-E) Live CD45$^+$ cells derived from lentivirally-transduced iPS cells on Day 26 of neutrophil differentiation were analyzed. Dead cells and CD45$^-$ cells were depleted using an autoMACS Pro separator (see *Methods*).

etry, a colony-forming assay, and cytostaining of HAX1-iPS cell-derived blood cells quantitatively demonstrated maturation arrest at the progenitor level and apoptotic predisposition due to low $\Delta\psi_m$ resulting in defective granulopoiesis, which were typically observed in SCN patients with *HAX1* gene deficiency. Thus, our culture system may serve as a novel experimental model and a platform for high-throughput screening of drugs for neutropenia in SCN with *HAX1* gene deficiency.

A colony-forming assay showed that the response to G-CSF administration correlated well with the responsiveness of SCN patients to G-CSF therapy. Defective granulopoiesis was recently reported in SCN-iPS cells with a mutation in *ELANE*.[24] Our data showing defective granulopoiesis and reduced response to G-CSF administration are generally consistent with this report. The slight differences in CFU-G/GM colony-forming potential between this previous study and the current study might be due to differences in the causative gene (*HAX1* or *ELANE*) or the culture system used for neutrophil differentiation, and/or to variation in the differentiation capabilities of the clones.

In our serum and feeder-free monolayer culture system, human ES and iPS cells differentiate into hematopoietic and endothelial cells via common KDR^+CD34^+ hemoangiogenic progenitors, which exist during early embryogenesis.[18] Therefore, emergence of abnormal granulopoiesis in this system suggests that disease onset might occur at early hematopoietic stage (yolk sac or fetal liver), which would have never been addressed with patient samples.

We also showed that *HAX1* cDNA transduction could reverse disease-related phenotypes such as abnormal granulopoiesis and apoptotic predisposition. Although little is known about the pathophysiology of SCN with *HAX1* gene deficiency, these results clearly indicated that a loss in HAX1 protein might be the primary cause of neutropenia. These results also indicated the possibility of using patient-derived iPS cells for gene therapy; however, there are technical difficulties that would preclude these cells from being used in a clinical setting. Lentiviral vectors that randomly integrate transgenes can affect the expression of related genes, including cancer-related genes.[25-28] To overcome these problems, we are required to select clones in which transgenes are integrated 'safe harbor' sites and highly expressed without perturbation of neighboring gene expression,[29] or to take the zinc finger nuclease-mediated gene targeting approach[30-32] specifically to a predesigned safe harbor site such as the *AAVS1* locus,[33] which has previously been shown to permit stable expression of transgenes with minimal effects on nearby genes.

The pluripotency of patient-derived iPS cells enables investigation of the pathophysiology of various organ abnormalities and/or dysfunctions. Many types of inherited bone marrow failure syndrome were characterized by multisystem developmental defects that affected the heart, kidney, skeletomuscular system, and central nervous system. Among these, neurological symptoms were frequently seen in SCN patients with *HAX1* gene deficiency,[19,23,34] suggesting that a loss in HAX1 may also affect neural development. Indeed, our patient also presented for epilepsy and severe delays in motor, cognitive, and intellectual development.[19] In patient-derived cells, $\Delta\psi_m$ was not reduced in undifferentiated iPS cells but was reduced in differentiated neutrophils. No marked abnormalities in teratoma formation by HAX1-iPS cells were observed. These results are partially consistent with the fact that SCN patients with a *HAX1* gene deficiency have only neutropenia and neurological symptoms, despite *HAX1* being a ubiquitously expressed gene.[6] Because some of these neurological symptoms cannot be reproduced in the currently available mouse model,[10] additional studies will be necessary to address the effects of *HAX1* on neural development by directed culture models of patient-derived iPS cells.

In conclusion, patient-derived iPS cell-derived myeloid cells were similar in disease presentation to SCN patients with *HAX1* gene deficiency, which could be reversed by gene correction in a novel *in vitro* neutrophil differentiation system. This culture system will serve as a new tool to facilitate disease modeling and drug screening for congenital neutrophil disorders.

Acknowledgments

The authors would like to thank Dr. Norio Nakatsuji for providing the human ES cell line KhES-1, Dr. Shinya Yamanaka for providing human iPS cell lines 201B6 and 253G4, and Dr. Hiroyuki Miyoshi for providing pCSII-EF-MCS. We are grate-

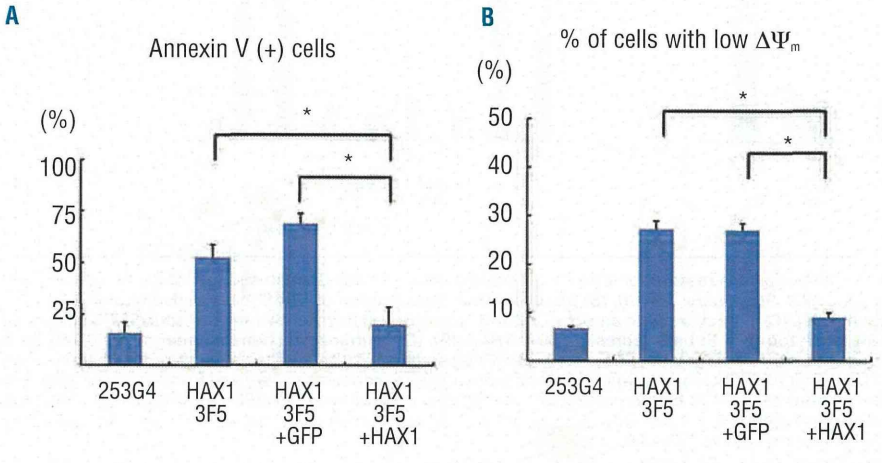

Figure 6. Lentiviral transduction of *HAX1* cDNA prevents HAX1-iPS cells being predisposed to undergo apoptosis. Annexin V assay (A) and mitochondrial membrane potential assay (B) of lentivirally-transduced iPS cell-derived cells on Day 26 of neutrophil differentiation. Cells gated on GFP^+ human $CD45^+$ were analyzed (n = 3; bars represent SDs; *P<0.05).